

# Distributionally Robust Beamforming and Estimation of Wireless Signals

Shixiong Wang, Wei Dai, and Geoffrey Ye Li, *Fellow, IEEE*

**Abstract**—This paper investigates signal estimation in wireless transmission from the perspective of statistical machine learning, where the transmitted signals may be from an integrated sensing and communication system; that is, 1) signals may be not only discrete constellation points but also arbitrary complex values; 2) signals may be spatially correlated. Particular attention is paid to handling various uncertainties such as the uncertainty of the transmitting signal covariance, the uncertainty of the channel matrix, the uncertainty of the channel noise covariance, the existence of channel impulse noises (i.e., outliers), and the limited sample size of pilots. To proceed, a distributionally robust machine learning framework that is insensitive to the above uncertainties is proposed for beamforming (at the receiver) and estimation of wireless signals, which reveals that channel estimation is not a necessary operation. For optimal linear estimation, the proposed framework includes several existing beamformers as special cases such as diagonal loading and eigenvalue thresholding. For optimal nonlinear estimation, estimators are limited in reproducing kernel Hilbert spaces and neural network function spaces, and corresponding uncertainty-aware solutions (e.g., kernelized diagonal loading) are derived. In addition, we prove that the ridge and kernel ridge regression methods in machine learning are distributionally robust against diagonal perturbation in feature covariance.

**Index Terms**—Wireless Transmission, Smart Antenna, Machine Learning, Robust Estimation, Robust Beamforming, Distributional Uncertainty, Channel Uncertainty, Limited Sample.

## I. INTRODUCTION

IN wireless transmission, detection and estimation of transmitted signals is of high importance, and beamforming at array receivers serves as a key signal-processing technique to suppress interference and environmental noises. The earliest beamforming solutions rely on the use of phase shifters (e.g., phased arrays) to steer and shape wave lobes, while advanced beamforming methods allow the employment of digital signal processing units, which introduce additional structural freedom (e.g., fully digital, hybrid, nonlinear, wideband) in beamformer design and significant performance improvement in signal recovery [1]–[3].

In traditional communication systems, transmitted signals are discrete points from constellations. Therefore, signal recovery, commonly referred to as *signal detection*, can be cast into a classification problem from the perspective of statistical machine learning, and the number of candidate

S. Wang, W. Dai, and G. Li are with the Department of Electrical and Electronic Engineering, Imperial College London, London SW7 2AZ, United Kingdom (E-mail: s.wang@u.nus.edu; wei.dai1@imperial.ac.uk; geoffrey.li@imperial.ac.uk).

This work is supported by the UK Department for Science, Innovation and Technology under the Future Open Networks Research Challenge project TUDOR (Towards Ubiquitous 3D Open Resilient Network).

classes is determined by the number of points in the employed constellation. Research in this stream includes, e.g., [4]–[9] as well as references therein, and the performance measure for signal detection is usually the misclassification rate (i.e., symbol error rate); representative algorithms encompass the maximum likelihood detector, the sphere decoding, etc. In another research stream, the signal recovery performance is evaluated using mean-squared errors (cf., signal-to-interference-plus-noise ratio), and the resultant signal recovery problem is commonly known as *signal estimation*, which can be considered as a regression problem from the perspective of statistical machine learning. By comparing the estimated symbols with the constellation points afterward, the detection of discrete symbols can be realized. For this case, till now, typical beamforming solutions include zero-forcing receivers, Wiener receivers (i.e., linear minimum mean-squared error receivers), Capon receivers (i.e., minimum variance distortionless response receivers), and nonlinear receivers such as neural-network receivers [10]–[12]. On the basis of these canonical approaches, variants such as robust beamformers working against the limited size of pilot samples and the uncertainty in steering vectors [13]–[18] have also been intensively reported; among these robust solutions, the diagonal loading method [19], [14, Eq. (11)] and the eigenvalue thresholding method [20], [14, Eq. (12)], etc., are popular due to their excellent balance in practical performance and technical simplicity.

Different from traditional paradigms, in emerging communication systems, e.g., integrated sensing and communication (ISAC) systems, transmitted signals may be arbitrary complex-valued symbols and spatially correlated [21]–[23]. As a result, mean-squared error is a preferred performance measure to investigate the *beamforming and estimation* problem of wireless signals, which is, therefore, the focus of this paper.

Although a large body of problems have been attacked in the area, the following signal-processing problems of beamforming and estimation in wireless transmission remain unsolved.

- 1) What is the relation between the signal-model-based approaches (e.g., Wiener and Capon receivers) and the data-driven approaches (e.g., deep-learning receivers)? In other words, how can we build a mathematically unified modeling framework to interpret all the existing digital beamformers?
- 2) In addition to the limited pilot size and the uncertainty in steering vectors, there exist other uncertainties in the signal model: the uncertainty in the transmitting signal covariance, the uncertainty of the communication channel matrix, the uncertainty of the channel noise covariance, and the presence of channel impulse noises (i.e., outliers).

Therefore, how can we handle all these types of uncertainties in a unified solution framework?

3) Existing literature mainly studied the robustness theory of linear beamformers against limited pilot size and the uncertainty in steering vectors [13]–[18]. However, how can we develop the theory of robust nonlinear beamformers against all the aforementioned uncertainties?

To this end, this paper designs a unified modeling and solution framework for beamforming and estimation of wireless signals, in consideration of the scarcity of the pilot data and the different uncertainties in the signal model.

### A. Contributions

The contributions of this paper can be summarized from the aspects of machine learning theory and wireless transmission theory.

In terms of machine learning theory, we give a theoretical justification and interpretation of the popular ridge regression and kernel ridge regression (i.e., quadratic loss function plus squared- $F$ -norm regularization) from the perspective of distributional robustness; see Theorems 2 and 3 (including the clarifications underneath them). To the knowledge of the authors, this is the first time to rigorously prove that the ridge and kernel ridge regression methods are distributionally robust, which enriches the theory of trustworthy machine learning.

In terms of wireless transmission theory, the contributions are outlined below.

- 1) We build a fundamentally theoretical framework for the beamforming and estimation of wireless signals from the perspective of statistical machine learning. In addition to the linear estimation method (i.e., beamforming at the receiver), nonlinear approaches (i.e., nonlinear beamforming) are also discussed in reproducing kernel Hilbert spaces and neural network function spaces. In particular, we reveal that channel estimation is not a necessary operation in beamforming and estimation of wireless signals. For details, see Subsection III-A.
- 2) The presented framework is particularly developed from the perspective of distributional robustness which can therefore combat the limited size of the training data set (i.e., limited pilot length) and several types of uncertainties in the wireless signal model such as the uncertainty in the transmitting power matrix, the uncertainty in the communication channel matrix, the existence of channel impulse noises (i.e., outliers), the uncertainty in the covariance matrix of channel noises, etc. For details, see Subsections III-B and III-C, and the technical developments in Sections IV and V.
- 3) Existing methods such as diagonal loading and eigenvalue thresholding are proven to be distributionally robust against the limited pilot size and all the aforementioned uncertainties in the wireless signal model. Extensions of diagonal loading and eigenvalue thresholding are proposed as well. Moreover, the kernelized diagonal loading and the kernelized eigenvalue thresholding methods are put forward for nonlinear estimation cases. For details, see Examples 1-7 and Subsections IV-B.

- 4) The distributionally robust beamforming and estimation problems across multiple frames, where channel conditions may change, are also investigated. For details, see Subsections IV-C and V-A2.

### B. Notations

The  $N$ -dimensional real (coordinate) space and complex (coordinate) space are denoted as  $\mathbb{R}^N$  and  $\mathbb{C}^N$ , respectively. Lowercase symbols (e.g.,  $\mathbf{x}$ ) denote vectors (column by default) and uppercase ones (e.g.,  $\mathbf{X}$ ) denote matrices. We use the Roman font for random quantities (e.g.,  $\mathbf{x}$ ,  $\mathbf{X}$ ) and the italic font for deterministic quantities (e.g.,  $\mathbf{x}$ ,  $\mathbf{X}$ ). Let  $\text{Re } \mathbf{X}$  be the real part of a complex quantity  $\mathbf{X}$  (a vector or matrix) and  $\text{Im } \mathbf{X}$  be the imaginary part of  $\mathbf{X}$ . For a vector  $\mathbf{x} \in \mathbb{C}^N$ , let

$$\underline{\mathbf{x}} := \begin{bmatrix} \text{Re } \mathbf{x} \\ \text{Im } \mathbf{x} \end{bmatrix} \in \mathbb{R}^{2N}$$

be the real-space representation of  $\mathbf{x}$ ; for a matrix  $\mathbf{H} \in \mathbb{C}^{N \times M}$ , let

$$\underline{\mathbf{H}} := \begin{bmatrix} \text{Re } \mathbf{H} \\ \text{Im } \mathbf{H} \end{bmatrix}, \quad \underline{\underline{\mathbf{H}}} := \begin{bmatrix} \text{Re } \mathbf{H} & -\text{Im } \mathbf{H} \\ \text{Im } \mathbf{H} & \text{Re } \mathbf{H} \end{bmatrix}$$

be the real-space representations of  $\mathbf{H}$  where  $\underline{\mathbf{H}} \in \mathbb{R}^{2N \times M}$  and  $\underline{\underline{\mathbf{H}}} \in \mathbb{R}^{2N \times 2M}$ . The running index set induced by an integer  $N$  is defined as  $[N] := \{1, 2, \dots, N\}$ . To concatenate matrices and vectors, MATLAB notations are used: i.e.,  $[\mathbf{A}, \mathbf{B}]$  for row stacking and  $[\mathbf{A}; \mathbf{B}]$  for column stacking. We let  $\mathbf{\Gamma}_M := [\mathbf{I}_M, \mathbf{J}_M] \in \mathbb{C}^{M \times 2M}$  where  $\mathbf{I}_M$  denotes the  $M$ -dimensional identity matrix,  $\mathbf{J}_M := j \cdot \mathbf{I}_M$ , and  $j$  denotes the imaginary unit. Let  $\mathcal{N}(\boldsymbol{\mu}, \boldsymbol{\Sigma})$  denote a real Gaussian distribution with mean  $\boldsymbol{\mu}$  and covariance  $\boldsymbol{\Sigma}$ . We use  $\mathcal{CN}(\mathbf{s}, \mathbf{P}, \mathbf{C})$  to denote a complex Gaussian distribution with mean  $\mathbf{s}$ , covariance  $\mathbf{P}$ , and pseudo-covariance  $\mathbf{C}$ ; if  $\mathbf{C}$  is not specified, we imply  $\mathbf{C} = \mathbf{0}$ . Throughout the paper, we use  $\mathbf{R}_{xs} := \mathbb{E} \mathbf{x} \mathbf{s}^H$  to denote the covariance matrix of  $\mathbf{x}$  and  $\mathbf{s}$ .

## II. PRELIMINARIES

We review two popular structured representation methods of nonlinear functions  $\phi : \mathbb{R}^N \rightarrow \mathbb{R}^M$ . More details can be seen in Appendix A of the online supplementary materials.

### A. Reproducing Kernel Hilbert Spaces

A reproducing kernel Hilbert space (RKHS)  $\mathcal{H}$  induced by the kernel function  $\text{ker} : \mathbb{R}^N \times \mathbb{R}^N \rightarrow \mathbb{R}$  and a collection of points  $\{\mathbf{x}_1, \mathbf{x}_2, \dots, \mathbf{x}_L\} \subset \mathbb{R}^N$  is a set of functions from  $\mathbb{R}^N$  to  $\mathbb{R}$ ;  $L$  may be infinite. Every function  $\phi : \mathbb{R}^N \rightarrow \mathbb{R}$  in the functional space  $\mathcal{H}$  can be represented by a linear combination [24, p. 539; Chap. 14]

$$\phi(\mathbf{x}) = \sum_{i=1}^L \omega_i \cdot \text{ker}(\mathbf{x}, \mathbf{x}_i), \quad \forall \mathbf{x} \in \mathbb{R}^N \quad (1)$$

where  $\{\omega_i\}_{i \in [L]}$  are the combination weights;  $\omega_i \in \mathbb{R}$  for every  $i \in [L]$ . The matrix form of (1) for  $M$ -multiple functions are

$$\phi(\mathbf{x}) := \begin{bmatrix} \phi_1(\mathbf{x}) \\ \phi_2(\mathbf{x}) \\ \vdots \\ \phi_M(\mathbf{x}) \end{bmatrix} = \mathbf{W} \cdot \varphi(\mathbf{x}) := \begin{bmatrix} \omega_1 \\ \omega_2 \\ \vdots \\ \omega_M \end{bmatrix} \cdot \varphi(\mathbf{x}), \quad (2)$$

where  $\omega_1, \omega_2, \dots, \omega_M \in \mathbb{R}^L$  are weight row-vectors for functions  $\phi_1(\mathbf{x}), \phi_2(\mathbf{x}), \dots, \phi_M(\mathbf{x})$ , respectively, and

$$\mathbf{W} := \begin{bmatrix} \omega_1 \\ \omega_2 \\ \vdots \\ \omega_M \end{bmatrix} \in \mathbb{R}^{M \times L}, \quad \varphi(\mathbf{x}) := \begin{bmatrix} \ker(\mathbf{x}, \mathbf{x}_1) \\ \ker(\mathbf{x}, \mathbf{x}_2) \\ \vdots \\ \ker(\mathbf{x}, \mathbf{x}_L) \end{bmatrix}. \quad (3)$$

Since a kernel function is pre-designed (i.e., fixed) for an RKHS  $\mathcal{H}$ , (2) suggests a  $\mathbf{W}$ -linear representation of  $\mathbf{x}$ -nonlinear functions  $\phi(\mathbf{x})$  in  $\mathcal{H}^M$ . Note that there exists a one-to-one correspondence between  $\phi$  and  $\mathbf{W}$ : for every  $\phi : \mathbb{R}^N \rightarrow \mathbb{R}^M$ , there exists a  $\mathbf{W} \in \mathbb{R}^{M \times L}$ , and vice versa.

### B. Neural Networks

Neural networks (NN) are another powerful tool to represent (i.e., approximate) nonlinear functions. A neural network function space (NNFS)  $\mathcal{K}$  characterizes (or parameterizes) a set of multi-input multi-output functions. Typical choices are multi-layer feed-forward neural networks, recurrent neural networks, etc. For beamforming and estimation of wireless signals, the multi-layer feed-forward neural networks are standard [10]–[12]. Suppose that we have  $R - 1$  hidden layers (so in total  $R + 1$  layers including one input layer and one output layer) and each layer  $r = 0, 1, \dots, R$  contains  $T_r$  neurons. To represent a function  $\phi : \mathbb{R}^N \rightarrow \mathbb{R}^M$ , for the input layer  $r = 0$  and output layer  $r = R$ , we have  $T_0 = N$  and  $T_R = M$ , respectively. Let the output of the  $r^{\text{th}}$  layer be  $\mathbf{y}_r \in \mathbb{R}^{T_r}$ . For every layer  $r$ , we have  $\mathbf{y}_r = \sigma_r(\mathbf{W}_r^{\circ} \cdot \mathbf{y}_{r-1} + \mathbf{b}_r)$  where  $\mathbf{W}_r^{\circ} \in \mathbb{R}^{T_r \times T_{r-1}}$  is the weight matrix,  $\mathbf{b}_r \in \mathbb{R}^{T_r}$  is the bias vector, and the multi-output function  $\sigma_r$  is the activation function which is entry-wise identical. Hence, every function  $\phi : \mathbb{R}^N \rightarrow \mathbb{R}^M$  in a NNFS can be recursively expressed as [25, Chap. 5], [26]

$$\begin{aligned} \phi(\mathbf{x}) &= \sigma_R(\mathbf{W}_R \cdot [\mathbf{y}_{R-1}(\mathbf{x}); 1]) \\ \mathbf{y}_r(\mathbf{x}) &= \sigma_r(\mathbf{W}_r \cdot [\mathbf{y}_{r-1}(\mathbf{x}); 1]), \quad r \in [R - 1] \\ \mathbf{y}_0(\mathbf{x}) &= \mathbf{x}, \end{aligned} \quad (4)$$

where  $\mathbf{W}_r := [\mathbf{W}_r^{\circ}, \mathbf{b}_r]$  for  $r \in [R]$ . Note that the activation functions can vary from one layer to another.

### III. PROBLEM FORMULATION

Consider a narrow-band wireless signal model

$$\mathbf{x} = \mathbf{H}\mathbf{s} + \mathbf{v} \quad (5)$$

where  $\mathbf{x} \in \mathbb{C}^N$  is the received signal,  $\mathbf{s} \in \mathbb{C}^M$  is the transmitted signal,  $\mathbf{H} \in \mathbb{C}^{N \times M}$  is the channel matrix, and  $\mathbf{v} \in \mathbb{C}^N$  is the zero-mean channel noise. The precoding operation (if exists) is integrated in  $\mathbf{H}$ . We assume  $\mathbf{x} \sim \mathcal{CN}(\mathbf{0}, \mathbf{R}_x, \mathbf{C}_x)$ ,  $\mathbf{s} \sim \mathcal{CN}(\mathbf{0}, \mathbf{R}_s, \mathbf{C}_s)$ , and  $\mathbf{v} \sim \mathcal{CN}(\mathbf{0}, \mathbf{R}_v)$ . The transmitted symbols  $\mathbf{s}$  have zero means, which may be not only discrete values from constellations such as quadrature amplitude modulation but also arbitrary symbols such as integrated sensing and communication (ISAC) signals. We consider  $L$  pilots/snapshots  $\mathbf{S} := (\mathbf{s}_1, \mathbf{s}_2, \dots, \mathbf{s}_L)$  in each frame, and the corresponding received symbols are  $\mathbf{X} := (\mathbf{x}_1, \mathbf{x}_2, \dots, \mathbf{x}_L)$  under the noise sequence  $(\mathbf{v}_1, \mathbf{v}_2, \dots, \mathbf{v}_L)$ ; in each frame,

$\mathbf{H}$  is assumed to be unchanged. For generality, we suppose that the covariances of the signal  $\mathbf{s}$  and the noise  $\mathbf{v}$  are  $\mathbf{R}_s := \mathbf{P} \succeq \mathbf{0}$  and  $\mathbf{R}_v := \mathbf{R} \succeq \mathbf{0}$ , respectively. Note that  $\mathbf{P}$  and  $\mathbf{R}$  may not be identity or diagonal matrices: i.e.,  $\mathbf{s}_i$  and  $\mathbf{s}_j$  can be correlated (e.g., in ISAC), so can be  $\mathbf{v}_i$  and  $\mathbf{v}_j$ , for every  $i, j \in [L]$ . Consider the real-space representation of the signal model (5) by stacking the real and imaginary components:

$$\underline{\mathbf{x}} = \underline{\mathbf{H}} \cdot \underline{\mathbf{s}} + \underline{\mathbf{v}}, \quad (6)$$

where  $\underline{\mathbf{x}} \in \mathbb{R}^{2N}$ ,  $\underline{\mathbf{H}} \in \mathbb{R}^{2N \times 2M}$ ,  $\underline{\mathbf{s}} \in \mathbb{R}^{2M}$ , and  $\underline{\mathbf{v}} \in \mathbb{R}^{2N}$ . The expressions of  $\mathbf{R}_{\underline{\mathbf{x}}} := \mathbb{E}\underline{\mathbf{x}}\underline{\mathbf{x}}^T$ ,  $\mathbf{R}_{\underline{\mathbf{s}}} := \mathbb{E}\underline{\mathbf{s}}\underline{\mathbf{s}}^T$ ,  $\mathbf{R}_{\underline{\mathbf{x}}\underline{\mathbf{s}}} := \mathbb{E}\underline{\mathbf{x}}\underline{\mathbf{s}}^T$ , and  $\mathbf{R}_{\underline{\mathbf{v}}} := \mathbb{E}\underline{\mathbf{v}}\underline{\mathbf{v}}^T$  can be readily obtained; see Appendix B of the online supplementary materials. Signal estimation in real spaces can be technically simpler than that in complex spaces.

### A. Optimal Estimation

1) *Optimal Nonlinear Estimation (Nonlinear Beamforming):* To recover  $\mathbf{s}$  using  $\mathbf{x}$ , we consider an estimator  $\hat{\mathbf{s}} := \phi(\mathbf{x})$  at the receiver where  $\phi : \mathbb{C}^N \rightarrow \mathbb{C}^M$  is a Borel-measurable function; note that  $\phi(\mathbf{x})$  may be nonlinear in general. The signal estimation problem at the receiver can be written as a statistical machine-learning problem under the joint data distribution  $\mathbb{P}_{\mathbf{x}, \mathbf{s}}$  of  $(\mathbf{x}, \mathbf{s})$ , that is,

$$\min_{\phi \in \mathcal{B}_{\mathbb{C}^N \rightarrow \mathbb{C}^M}} \text{Tr} \mathbb{E}_{\mathbf{x}, \mathbf{s}} [\phi(\mathbf{x}) - \mathbf{s}] [\phi(\mathbf{x}) - \mathbf{s}]^H, \quad (7)$$

where  $\mathcal{B}_{\mathbb{C}^N \rightarrow \mathbb{C}^M}$  contains all Borel-measurable estimators from  $\mathbb{C}^N$  to  $\mathbb{C}^M$ . In what follows, we omit the notational dependence on  $\mathbb{C}^N$  and  $\mathbb{C}^M$ , and use  $\mathcal{B}$  as a shorthand. The optimal estimator, in the sense of minimum mean-squared error, is known as the conditional mean of  $\mathbf{s}$  given  $\mathbf{x}$ , i.e.,

$$\hat{\mathbf{s}} = \phi(\mathbf{x}) = \mathbb{E}(\mathbf{s} | \mathbf{x}), \quad (8)$$

Therefore, we have  $\mathbf{s} = \hat{\mathbf{s}} + \mathbf{e}$ , that is,

$$\mathbf{s} = \phi(\mathbf{x}) + \mathbf{e} \quad (9)$$

where  $\mathbf{e}$  denotes the signal's estimation error; (9) implies that the estimation problem of  $\mathbf{s}$  from  $\mathbf{x}$  can be seen as a nonlinear regression problem of the collected data pairs  $\{(\mathbf{x}_1, \mathbf{s}_1), (\mathbf{x}_2, \mathbf{s}_2), \dots, (\mathbf{x}_L, \mathbf{s}_L)\}$ . In literature, some authors refer to nonlinear estimator  $\phi(\cdot)$  as a nonlinear beamformer. Usually, it is technically complicated to find the optimal  $\phi(\cdot)$  from the whole space  $\mathcal{B}$  of Borel-measurable functions. Therefore, in practice, we may find the optimal approximation of  $\phi(\cdot)$  in an RKHS  $\mathcal{H}$  or a NNFS  $\mathcal{K}$ ; note that  $\mathcal{H}$  and  $\mathcal{K}$  are two subspaces of  $\mathcal{B}$ . However, both  $\mathcal{H}$  and  $\mathcal{K}$  are sufficiently rich in the sense of being able to include all continuous bounded functions.

2) *Optimal Linear Estimation (Beamforming):* When  $\mathbf{x}$  and  $\mathbf{s}$  are jointly Gaussian (e.g., when  $\mathbf{s}$  and  $\mathbf{v}$  are jointly Gaussian), the optimal estimator  $\phi$  is linear in  $\mathbf{x}$ :

$$\hat{\mathbf{s}} = \mathbf{W}\mathbf{x}, \quad (10)$$

where  $\mathbf{W} \in \mathbb{C}^{M \times N}$  is called a smart antenna or a beamformer. In this linear case, (7) reduces to the usual Wiener–Hopf beamforming problem

$$\min_{\mathbf{W}} \text{Tr} \mathbb{E}_{\mathbf{x}, \mathbf{s}} [\mathbf{W}\mathbf{x} - \mathbf{s}] [\mathbf{W}\mathbf{x} - \mathbf{s}]^H, \quad (11)$$

that is,

$$\min_{\mathbf{W}} \text{Tr} [\mathbf{W} \mathbf{R}_x \mathbf{W}^H - \mathbf{W} \mathbf{R}_{xs} - \mathbf{R}_{xs}^H \mathbf{W}^H + \mathbf{R}_s], \quad (12)$$

where  $\mathbf{R}_x := \mathbb{E} \mathbf{x} \mathbf{x}^H \in \mathbb{C}^{N \times N}$ ,  $\mathbf{R}_s := \mathbb{E} \mathbf{s} \mathbf{s}^H = \mathbf{P} \in \mathbb{C}^{M \times M}$ , and  $\mathbf{R}_{xs} := \mathbb{E} \mathbf{x} \mathbf{s}^H \in \mathbb{C}^{N \times M}$ . Denote  $\mathbf{R}_v := \mathbb{E} \mathbf{v} \mathbf{v}^H = \mathbf{R} \in \mathbb{C}^{N \times N}$ . Since  $\mathbf{R}_x = \mathbf{H} \mathbf{R}_s \mathbf{H}^H + \mathbf{R}_v = \mathbf{H} \mathbf{P} \mathbf{H}^H + \mathbf{R}$  and  $\mathbf{R}_{xs} = \mathbf{H} \mathbf{R}_s + \mathbf{R}_{sv} = \mathbf{H} \mathbf{P}$ , the solution of (12), or (11), is

$$\begin{aligned} \mathbf{W}_{\text{Wiener}}^* &= \mathbf{R}_{xs}^H \mathbf{R}_x^{-1} \\ &= \mathbf{P} \mathbf{H}^H [\mathbf{H} \mathbf{P} \mathbf{H}^H + \mathbf{R}]^{-1}, \end{aligned} \quad (13)$$

which is known as the Wiener beamformer. With an additional constraint  $\mathbf{W} \mathbf{H} = \mathbf{I}_M$  (i.e., distortionless response), (12) gives the Capon beamformer. Both the Wiener beamformer and the Capon beamformer maximize the output signal-to-interference-plus-noise ratio (SINR); hence, both are optimal in the sense of maximum output SINR. No matter whether  $\mathbb{P}_{\mathbf{x}, \mathbf{s}}$  is Gaussian or not, (11) or (12) gives the **optimal linear beamformer** in the sense of maximizing the output SINR among all linear beamformers.

3) *Role of Channel Estimation:* As we can see from (7) and (11), channel estimation is not a necessary step in the estimation of wireless signals. The only necessary element, from the perspectives of statistical inference and machine learning, is the joint distribution  $\mathbb{P}_{\mathbf{x}, \mathbf{s}}$  of the received signal  $\mathbf{x}$  and the transmitted signal  $\mathbf{s}$ . Therefore, the following two points can be highlighted.

- 1) If the joint distribution  $\mathbb{P}_{\mathbf{x}, \mathbf{s}}$  is non-Gaussian, we just need to learn the mapping  $\phi$  using (7).
- 2) If the joint distribution  $\mathbb{P}_{\mathbf{x}, \mathbf{s}}$  is (or assumed to be) Gaussian, we just need to learn the covariance matrices  $\mathbf{R}_{xs}$  and  $\mathbf{R}_x$ ; cf. (13). If, further, the channel matrix  $\mathbf{H}$  is known,  $\mathbf{R}_{xs}$  and  $\mathbf{R}_x$  can be expressed using  $\mathbf{H}$ .

Since  $\mathbf{H}$  can be an integrated channel after precoding (e.g.,  $\mathbf{H} := \mathbf{H}_0 \mathbf{B}_p$  where  $\mathbf{H}_0$  denotes the physical channel and  $\mathbf{B}_p$  the precoder), the knowledge of the precoding operation is also unnecessary for receivers when estimating the transmitted signals. This is practically beneficial because we do not need to build an exact channel model and then accurately estimate the channel, which is challenging especially when the channel statistics are time-varying or the channel noise is non-Gaussian and non-stationary; cf. [10].

### B. Issue of Distributional Uncertainty

In practice, the true joint distribution  $\mathbb{P}_{\mathbf{x}, \mathbf{s}}$  is unknown but we have samples  $\{(\mathbf{x}_1, \mathbf{s}_1), (\mathbf{x}_2, \mathbf{s}_2), \dots, (\mathbf{x}_L, \mathbf{s}_L)\}$  from  $\mathbb{P}_{\mathbf{x}, \mathbf{s}}$ . Hence, the beamforming and estimation problem of wireless signals is a data-driven statistical inference (i.e., statistical machine learning) problem. We let

$$\hat{\mathbb{P}}_{\mathbf{x}, \mathbf{s}} := \frac{1}{L} \sum_{i=1}^L \delta_{(\mathbf{x}_i, \mathbf{s}_i)} \quad (14)$$

denote the empirical distribution supported on the  $L$  collected data  $\{(\mathbf{x}_i, \mathbf{s}_i)\}_{i \in [L]}$ , where  $\delta_{(\mathbf{x}_i, \mathbf{s}_i)}$  denotes the Dirac distribution (i.e., point-mass distribution) centered on  $(\mathbf{x}_i, \mathbf{s}_i)$ ; note that  $\hat{\mathbb{P}}_{\mathbf{x}, \mathbf{s}}$  is a discrete distribution. If we use the estimated joint distribution  $\hat{\mathbb{P}}_{\mathbf{x}, \mathbf{s}}$  as a surrogate for the true joint distribution

$\mathbb{P}_{\mathbf{x}, \mathbf{s}}$ , (7) becomes the conventional empirical risk minimization (ERM)  $\min_{\phi \in \mathcal{B}} \text{Tr} \mathbb{E}_{(\mathbf{x}, \mathbf{s}) \sim \hat{\mathbb{P}}_{\mathbf{x}, \mathbf{s}}} [\phi(\mathbf{x}) - \mathbf{s}] [\phi(\mathbf{x}) - \mathbf{s}]^H$ , i.e.,

$$\min_{\phi \in \mathcal{B}} \text{Tr} \frac{1}{L} \sum_{i=1}^L [\phi(\mathbf{x}_i) - \mathbf{s}_i] [\phi(\mathbf{x}_i) - \mathbf{s}_i]^H. \quad (15)$$

Likewise, (12) become the conventional beamforming problem

$$\min_{\mathbf{W}} \text{Tr} [\mathbf{W} \hat{\mathbf{R}}_x \mathbf{W}^H - \mathbf{W} \hat{\mathbf{R}}_{xs} - \hat{\mathbf{R}}_{xs}^H \mathbf{W}^H + \hat{\mathbf{R}}_s], \quad (16)$$

where  $\hat{\mathbf{R}}_x$ ,  $\hat{\mathbf{R}}_{xs}$ , and  $\hat{\mathbf{R}}_s$  are the training-sample-estimated (i.e., nominal) values of  $\mathbf{R}_x$ ,  $\mathbf{R}_{xs}$ , and  $\mathbf{R}_s$ , respectively.

There exists the distributional difference between the sample-defined nominal distribution  $\hat{\mathbb{P}}_{\mathbf{x}, \mathbf{s}}$  and true data-generating distribution  $\mathbb{P}_{\mathbf{x}, \mathbf{s}}$  due to the limited size of the training data set (i.e., limited pilot length), the uncertainty in the transmitting power matrix, the uncertainty in the channel matrix (e.g., the channel may be time-selective in a frame), the existence of channel impulse noises (i.e., outliers), the uncertainty in channel noise covariance, etc. From the perspective of applied statistics and machine learning, the distributional difference between  $\hat{\mathbb{P}}_{\mathbf{x}, \mathbf{s}}$  and  $\mathbb{P}_{\mathbf{x}, \mathbf{s}}$  (i.e., the distributional uncertainty of  $\hat{\mathbb{P}}_{\mathbf{x}, \mathbf{s}}$  compared to  $\mathbb{P}_{\mathbf{x}, \mathbf{s}}$ ) may cause significant performance degradation of (15) compared to (7), so is the performance deterioration of (16) compared to (12). For extensive reading on this point, see Appendix C of the online supplementary materials. Therefore, to reduce the adverse effect introduced by the distributional uncertainty in  $\hat{\mathbb{P}}_{\mathbf{x}, \mathbf{s}}$ , a new surrogate of (7) rather than the sample-averaged approximation in (15) is expected.

### C. Distributionally Robust Estimation

To combat the distributional uncertainty in  $\hat{\mathbb{P}}_{\mathbf{x}, \mathbf{s}}$ , we consider the distributionally robust counterpart of (7)

$$\min_{\phi \in \mathcal{B}} \max_{\mathbb{P}_{\mathbf{x}, \mathbf{s}} \in \mathcal{U}_{\mathbf{x}, \mathbf{s}}} \text{Tr} \mathbb{E}_{\mathbf{x}, \mathbf{s}} [\phi(\mathbf{x}) - \mathbf{s}] [\phi(\mathbf{x}) - \mathbf{s}]^H, \quad (17)$$

where  $\mathcal{U}_{\mathbf{x}, \mathbf{s}}$ , called a distributional uncertainty set, contains a collection of distributions that are close to the nominal distribution (i.e., the sample-estimated distribution)  $\hat{\mathbb{P}}_{\mathbf{x}, \mathbf{s}}$ , i.e.,

$$\mathcal{U}_{\mathbf{x}, \mathbf{s}} := \{\mathbb{P}_{\mathbf{x}, \mathbf{s}} | d(\mathbb{P}_{\mathbf{x}, \mathbf{s}}, \hat{\mathbb{P}}_{\mathbf{x}, \mathbf{s}}) \leq \epsilon\}, \quad (18)$$

where  $d(\cdot, \cdot)$  denotes a distance between two distributions. Since  $\hat{\mathbb{P}}_{\mathbf{x}, \mathbf{s}}$  is discrete and  $\mathbb{P}_{\mathbf{x}, \mathbf{s}}$  can be continuous, the Wasserstein distance [27, Def. 2] and the maximum mean discrepancy (MMD) distance [28, Def. 2.1] are the usual choices of  $d(\cdot, \cdot)$  to construct  $\mathcal{U}_{\mathbf{x}, \mathbf{s}}$ . For extensive reading on the Wasserstein and MMD distances, see Appendix D of the online supplementary materials. When  $\epsilon = 0$ , (17) reduces to (15). If  $\mathcal{U}_{\mathbf{x}, \mathbf{s}}$  contains only Gaussian distributions, (17) is particularized to

$$\begin{aligned} \min_{\mathbf{W}} \max_{\mathbf{R}_x, \mathbf{R}_{xs}, \mathbf{R}_s} & \text{Tr} [\mathbf{W} \mathbf{R}_x \mathbf{W}^H - \mathbf{W} \mathbf{R}_{xs} - \mathbf{R}_{xs}^H \mathbf{W}^H + \mathbf{R}_s] \\ \text{s.t.} & d_1(\mathbf{R}_x, \hat{\mathbf{R}}_x) \leq \epsilon_1, \\ & d_2(\mathbf{R}_{xs}, \hat{\mathbf{R}}_{xs}) \leq \epsilon_2, \\ & d_3(\mathbf{R}_s, \hat{\mathbf{R}}_s) \leq \epsilon_3, \\ & \mathbf{R}_x \succeq \mathbf{0}, \mathbf{R}_x = \mathbf{R}_x^H, \\ & \mathbf{R}_s \succeq \mathbf{0}, \mathbf{R}_s = \mathbf{R}_s^H, \end{aligned} \quad (19)$$

because every zero-mean complex Gaussian distribution is uniquely characterized by its covariance and pseudo-covariance, but in beamforming, we do not consider pseudo-covariances; cf. (13);  $d_1$ ,  $d_2$ , and  $d_3$  are matrix similarity measures (e.g., matrix distances);  $\epsilon_1 \geq 0$ ,  $\epsilon_2 \geq 0$ , and  $\epsilon_3 \geq 0$  are uncertainty quantification parameters. When  $\epsilon_1 = \epsilon_2 = \epsilon_3 = 0$ , (19) reduces to (16). The fact below characterizes the performance of the distributionally robust estimators.

*Fact 1:* Suppose that the true distribution  $\mathbb{P}_{0,\mathbf{x},\mathbf{s}}$  of  $(\mathbf{x}, \mathbf{s})$  is included in  $\mathcal{U}_{\mathbf{x},\mathbf{s}}$ ; for notational clarity, we hereafter distinguish  $\mathbb{P}_{0,\mathbf{x},\mathbf{s}}$  from  $\mathbb{P}_{\mathbf{x},\mathbf{s}}$ . The true estimation error evaluated at  $\mathbb{P}_{0,\mathbf{x},\mathbf{s}}$

$$\min_{\phi \in \mathcal{B}} \text{Tr} \mathbb{E}_{(\mathbf{x}, \mathbf{s}) \sim \mathbb{P}_{0,\mathbf{x},\mathbf{s}}} [\phi(\mathbf{x}) - \mathbf{s}] [\phi(\mathbf{x}) - \mathbf{s}]^H \quad (20)$$

is upper bounded by the worst-case estimation error (17). Therefore, by diminishing the upper bound in (17), the true estimation error (20) can also be reduced. However, the conventional empirical estimation error (15) cannot upper bound the true estimation error (20). This performance guarantee is the benefit of considering the distributionally robust method (17). Due to the weak convergence property of the empirical distribution to the true data-generating distribution, that is,  $d(\mathbb{P}_{0,\mathbf{x},\mathbf{s}}, \hat{\mathbb{P}}_{\mathbf{x},\mathbf{s}}) \rightarrow 0$  as the sample size  $L \rightarrow \infty$ , there exists  $\epsilon$  in (18) for every  $L$ , such that  $\mathbb{P}_{0,\mathbf{x},\mathbf{s}}$  is included in  $\mathcal{U}_{\mathbf{x},\mathbf{s}}$  in  $\mathbb{P}_{0,\mathbf{x},\mathbf{s}}^L$ -probability ( $L$ -fold product measure of  $\mathbb{P}_{0,\mathbf{x},\mathbf{s}}$ ).  $\square$

#### IV. DISTRIBUTIONALLY ROBUST LINEAR ESTIMATION

Due to several practical benefits of linear estimation, for example, the simplicity of hardware structures, the clarity of physical meaning (i.e., constructive and destructive interference through beamforming), and the easiness of computations, investigating distributionally robust linear estimation problems is important. This section particularly studies Problem (19).

##### A. General Framework and Concrete Examples

The following lemma equivalently transforms Problem (19).

*Lemma 1:* Problem (19) is equivalent to

$$\begin{aligned} \max_{\mathbf{R}_x, \mathbf{R}_{xs}, \mathbf{R}_s} \min_{\mathbf{W}} \quad & \text{Tr} [\mathbf{W} \mathbf{R}_x \mathbf{W}^H - \mathbf{W} \mathbf{R}_{xs} - \mathbf{R}_{xs}^H \mathbf{W}^H + \mathbf{R}_s] \\ \text{s.t.} \quad & d_1(\mathbf{R}_x, \hat{\mathbf{R}}_x) \leq \epsilon_1, \\ & d_2(\mathbf{R}_{xs}, \hat{\mathbf{R}}_{xs}) \leq \epsilon_2, \\ & d_3(\mathbf{R}_s, \hat{\mathbf{R}}_s) \leq \epsilon_3, \\ & \mathbf{R}_x \succeq \mathbf{0}, \mathbf{R}_x = \mathbf{R}_x^H, \\ & \mathbf{R}_s \succeq \mathbf{0}, \mathbf{R}_s = \mathbf{R}_s^H, \end{aligned} \quad (21)$$

provided that  $d_1(\mathbf{R}_x, \hat{\mathbf{R}}_x)$  is convex in  $\mathbf{R}_x$ ,  $d_2(\mathbf{R}_{xs}, \hat{\mathbf{R}}_{xs})$  is convex in  $\mathbf{R}_{xs}$ , and  $d_3(\mathbf{R}_s, \hat{\mathbf{R}}_s)$  is convex in  $\mathbf{R}_s$ . Problem (19) is further equivalent to

$$\begin{aligned} \max_{\mathbf{R}_x, \mathbf{R}_{xs}, \mathbf{R}_s} \quad & \text{Tr} [-\mathbf{R}_{xs}^H \mathbf{R}_x^{-1} \mathbf{R}_{xs} + \mathbf{R}_s] \\ \text{s.t.} \quad & d_1(\mathbf{R}_x, \hat{\mathbf{R}}_x) \leq \epsilon_1, \\ & d_2(\mathbf{R}_{xs}, \hat{\mathbf{R}}_{xs}) \leq \epsilon_2, \\ & d_3(\mathbf{R}_s, \hat{\mathbf{R}}_s) \leq \epsilon_3, \\ & \mathbf{R}_x \succeq \mathbf{0}, \mathbf{R}_x = \mathbf{R}_x^H, \\ & \mathbf{R}_s \succeq \mathbf{0}, \mathbf{R}_s = \mathbf{R}_s^H. \end{aligned} \quad (22)$$

*Proof:* This is by the Sion's minimax theorem. Note that the objective function is convex in  $\mathbf{W}$  and linear (thus

concave) in both  $\mathbf{R}_x$ ,  $\mathbf{R}_{xs}$ , and  $\mathbf{R}_s$ . Note also that complex Euclidean spaces are linear topological spaces. For every given  $\mathbf{R}_x$  and  $\mathbf{R}_{xs}$ , the inner minimization sub-problem of (21) is solved by the Wiener beamformer  $\mathbf{W}_{\text{Wiener}}^* = \mathbf{R}_{xs}^H \mathbf{R}_x^{-1}$ , which transforms (21) to 22. This completes the proof.  $\square$

Let

$$f(\mathbf{R}_x) := \text{Tr} [-\mathbf{R}_{xs}^H \mathbf{R}_x^{-1} \mathbf{R}_{xs} + \mathbf{R}_s] \quad (23)$$

denote the objective function of (22) in terms of  $\mathbf{R}_x$ , i.e., a matrix-valued function of  $\mathbf{R}_x \succeq \mathbf{0}$ . The following theorem shows the monotonicity of  $f(\mathbf{R}_x)$  in  $\mathbf{R}_x$ .

*Theorem 1:* Function  $f(\mathbf{R}_x)$  in (23) is monotonically increasing in  $\mathbf{R}_x$ : i.e., if  $\mathbf{R}_{x,1} \succeq \mathbf{R}_{x,2}$ , we have  $f(\mathbf{R}_{x,1}) \geq f(\mathbf{R}_{x,2})$ .

*Proof:* See Appendix E of the online supplementary materials.  $\square$

Theorem 1 implies that if  $\mathbf{R}_x^* \succeq \mathbf{R}_x$  for all  $\mathbf{R}_x$  such that  $d_1(\mathbf{R}_x, \hat{\mathbf{R}}_x) \leq \epsilon_1$ , then  $\mathbf{R}_x^*$  is a maximizer of Problem (22).

It is also straightforward to see that if  $\mathbf{R}_s^* \succeq \mathbf{R}_s$  for all  $\mathbf{R}_s$  such that  $d_3(\mathbf{R}_s, \hat{\mathbf{R}}_s) \leq \epsilon_3$ , then  $\mathbf{R}_s^*$  is a maximizer of Problem (22).

The objective function of Problem (22) is negative-definite concave in  $\text{vec}(\mathbf{R}_{xs})$ . Therefore, Problem (22) can be readily solved using any first-order method such as the projected gradient ascent method; the gradient of the objective function with respect to  $\mathbf{R}_{xs}$  is  $-2\mathbf{R}_x^{-1} \mathbf{R}_{xs}$ . When we do not study the uncertainty in the channel  $\mathbf{H}$  (because this paper does not intend to explicitly estimate the channel matrix), since  $\mathbf{R}_{xs} = \mathbf{H} \mathbf{P}$ , the uncertainty of  $\mathbf{R}_{xs}$  is induced by the uncertainty of the covariance  $\mathbf{P} := \mathbf{R}_s$  of the transmitted signal  $\mathbf{s}$ . As a result, we can study the uncertainty in  $\mathbf{P}$  instead.

If the uncertainties in  $\mathbf{R}_x$  and  $\mathbf{R}_{xs}$  are induced by the uncertainties in the transmitted signal covariance  $\mathbf{P} := \mathbf{R}_s$  and the noise covariance  $\mathbf{R} := \mathbf{R}_v$ , Problem (22) can be explicitly written as

$$\begin{aligned} \max_{\mathbf{P}, \mathbf{R}} \quad & \text{Tr} [\mathbf{P} - \mathbf{P} \mathbf{H}^H (\mathbf{H} \mathbf{P} \mathbf{H}^H + \mathbf{R})^{-1} \mathbf{H} \mathbf{P}] \\ \text{s.t.} \quad & d_4(\mathbf{P}, \hat{\mathbf{P}}) \leq \epsilon_4, \\ & d_5(\mathbf{R}, \hat{\mathbf{R}}) \leq \epsilon_5, \\ & \mathbf{P} \succeq \mathbf{0}, \mathbf{R} \succeq \mathbf{0}, \\ & \mathbf{P} = \mathbf{P}^H, \mathbf{R} = \mathbf{R}^H, \end{aligned} \quad (24)$$

for some similarity measures  $d_4$  and  $d_5$  and nonnegative scalars  $\epsilon_4$  and  $\epsilon_5$ . For every  $(\mathbf{P}, \mathbf{R})$ , the associated beamformer is given in (13). When the uncertainty in the channel matrix must be investigated, we can consider

$$\begin{aligned} \max_{\mathbf{H}} \quad & \text{Tr} [\mathbf{P} - \mathbf{P} \mathbf{H}^H (\mathbf{H} \mathbf{P} \mathbf{H}^H + \mathbf{R})^{-1} \mathbf{H} \mathbf{P}] \\ \text{s.t.} \quad & d_6(\mathbf{H}, \hat{\mathbf{H}}) \leq \epsilon_6, \end{aligned} \quad (25)$$

which is not a semi-definite program. In addition, the gradient of the objective function with respect to  $\mathbf{H}$  is complicated to obtain. Hence, a solution method should be tailored.

Below we provide some concrete examples to showcase the practical usefulness and applications of (22) and (24).

*Example 1 (Diagonally Loaded Beamforming):* Consider the uncertainty in  $\mathbf{R}_x$ . Suppose  $d_1(\mathbf{R}_x, \hat{\mathbf{R}}_x) \leq \epsilon_1$  is particularized as

$$\hat{\mathbf{R}}_x - \epsilon_1 \mathbf{I}_N \preceq \mathbf{R}_x \preceq \hat{\mathbf{R}}_x + \epsilon_1 \mathbf{I}_N; \quad (26)$$

that is,  $\mathbf{R}_x$  lies in the diagonal  $\epsilon_1$ -neighbourhood (i.e., diagonal  $\epsilon_1$ -perturbation) of  $\hat{\mathbf{R}}_x$ . By Theorem 1, we have the distributionally robust beamformer

$$\begin{aligned} \mathbf{W}_{\text{DR-DL}}^* &= \mathbf{R}_{xs}^H [\hat{\mathbf{R}}_x + \epsilon_1 \mathbf{I}_N]^{-1} \\ &= \mathbf{P} \mathbf{H}^H [\mathbf{H} \mathbf{P} \mathbf{H}^H + \hat{\mathbf{R}} + \epsilon_1 \mathbf{I}_N]^{-1}, \end{aligned} \quad (27)$$

which is known as the loaded sample matrix inversion method or the diagonal loading method [19], [14, Eq. (11)]. Note that when  $\mathbf{R}_{xs}$  is accurate,  $\mathbf{P}$  and  $\mathbf{H}$  are accurate. Therefore, the uncertainty in  $\hat{\mathbf{R}}_x$  comes from the uncertainty in  $\hat{\mathbf{R}}$ .  $\square$

Diagonally loaded beamforming can handle the scarcity of pilot data: When  $L$  is not sufficiently large, the estimate  $\hat{\mathbf{R}}_x$  of  $\mathbf{R}_x$  would be significantly unreliable; cf. Subsection III-B.

*Example 2 (Distributionally Robust Capon Beamforming):* We consider a distributionally robust Capon beamforming problem:

$$\begin{aligned} \min_{\mathbf{W}} \max_{\mathbf{R}_x} \quad & \text{Tr} [\mathbf{W} \mathbf{R}_x \mathbf{W}^H - 2\mathbf{P} + \mathbf{R}_s] \\ \text{s.t.} \quad & \mathbf{W} \mathbf{H} = \mathbf{I}_M, \\ & \hat{\mathbf{R}}_x - \epsilon_1 \mathbf{I}_N \preceq \mathbf{R}_x \preceq \hat{\mathbf{R}}_x + \epsilon_1 \mathbf{I}_N, \\ & \mathbf{R}_x \succeq \mathbf{0}, \quad \mathbf{R}_x = \mathbf{R}_x^H, \end{aligned}$$

which is equivalent, in the sense of the same minimizer, to

$$\begin{aligned} \min_{\mathbf{W}} \max_{\mathbf{R}_x} \quad & \text{Tr} [\mathbf{W} \mathbf{R}_x \mathbf{W}^H] \\ \text{s.t.} \quad & \mathbf{W} \mathbf{H} = \mathbf{I}_M, \\ & \hat{\mathbf{R}}_x - \epsilon_1 \mathbf{I}_N \preceq \mathbf{R}_x \preceq \hat{\mathbf{R}}_x + \epsilon_1 \mathbf{I}_N, \\ & \mathbf{R}_x \succeq \mathbf{0}, \quad \mathbf{R}_x = \mathbf{R}_x^H. \end{aligned}$$

According to Lemma 1 and Theorem 1, the above display is further equivalent to

$$\begin{aligned} \min_{\mathbf{W}} \quad & \text{Tr} [\mathbf{W} (\hat{\mathbf{R}}_x + \epsilon_1 \mathbf{I}_N) \mathbf{W}^H] \\ \text{s.t.} \quad & \mathbf{W} \mathbf{H} = \mathbf{I}_M, \end{aligned}$$

that is,

$$\begin{aligned} \min_{\mathbf{W}} \quad & \text{Tr} [\mathbf{W} \hat{\mathbf{R}}_x \mathbf{W}^H] + \epsilon_1 \cdot \text{Tr} [\mathbf{W} \mathbf{W}^H] \\ \text{s.t.} \quad & \mathbf{W} \mathbf{H} = \mathbf{I}_M. \end{aligned}$$

The above formulation is the squared- $F$ -norm-regularized Capon beamformer [14, Eq. (10)] whose solution is

$$\begin{aligned} \mathbf{W}_{\text{DR-Capon}}^* &= [\mathbf{H}^H (\hat{\mathbf{R}}_x + \epsilon_1 \mathbf{I}_N)^{-1} \mathbf{H}]^{-1}, \\ &\quad \mathbf{H}^H (\hat{\mathbf{R}}_x + \epsilon_1 \mathbf{I}_N)^{-1}, \end{aligned} \quad (28)$$

which is the diagonally loaded Capon beamformer.  $\square$

*Example 3 (Eigenvalue Thresholding):* Suppose that  $\hat{\mathbf{R}}_x$  admits the eigenvalues of  $\text{diag}\{\lambda_1, \lambda_2, \dots, \lambda_N\}$  in descending order and the eigenvectors in  $\mathbf{Q}$  (columns). Let  $0 \leq \mu \leq 1$  be a shrinking coefficient. If we assume  $\mathbf{R}_x \preceq \hat{\mathbf{R}}_{x,\text{thr}}$  where

$$\hat{\mathbf{R}}_{x,\text{thr}} := \mathbf{Q} \begin{bmatrix} \lambda_1 & \max\{\mu\lambda_1, \lambda_2\} & & \\ & \ddots & \ddots & \\ & & \ddots & \max\{\mu\lambda_1, \lambda_N\} \end{bmatrix} \mathbf{Q}^{-1}, \quad (29)$$

we have the distributionally robust beamformer

$$\mathbf{W}_{\text{DR-ET}}^* = \mathbf{R}_{xs}^H \hat{\mathbf{R}}_{x,\text{thr}}^{-1}, \quad (30)$$

which is known as the eigenvalue thresholding method [20], [14, Eq. (12)].  $\square$

In the next example, we consider the uncertainties in covariance  $\mathbf{P}$  of transmitted signal  $\mathbf{s}$  and covariance  $\mathbf{R}$  of channel noise  $\mathbf{v}$ .

*Example 4 (Distributionally Robust Beamforming for Uncertain  $\mathbf{P}$  and  $\mathbf{R}$ ):* Consider Problem (24), as well as the uncertainties in covariance  $\mathbf{P}$  of transmitted signal  $\mathbf{s}$  and covariance  $\mathbf{R}$  of channel noise  $\mathbf{v}$ . Since the objective function of (24) is increasing in both  $\mathbf{P}$  and  $\mathbf{R}$ ,<sup>1</sup> if

$$\hat{\mathbf{P}} - \epsilon_4 \mathbf{I}_M \preceq \mathbf{P} \preceq \hat{\mathbf{P}} + \epsilon_4 \mathbf{I}_M,$$

we have a distributionally robust beamformer

$$\begin{aligned} \mathbf{W}_{\text{DR-P}}^* &= (\hat{\mathbf{P}} + \epsilon_4 \mathbf{I}_M) \mathbf{H}^H [\mathbf{H} (\hat{\mathbf{P}} + \epsilon_4 \mathbf{I}_M) \mathbf{H}^H + \mathbf{R}]^{-1} \\ &= (\hat{\mathbf{P}} + \epsilon_4 \mathbf{I}_M) \mathbf{H}^H [\mathbf{H} \hat{\mathbf{P}} \mathbf{H}^H + \mathbf{R} + \epsilon_4 \mathbf{H} \mathbf{H}^H]^{-1}, \end{aligned} \quad (31)$$

which is tantamount to the diagonally loaded beamformer but loaded by the squared channel matrix  $\mathbf{H} \mathbf{H}^H$  rather than the identity matrix. On the other hand, if

$$\hat{\mathbf{R}} - \epsilon_5 \mathbf{I}_N \preceq \mathbf{R} \preceq \hat{\mathbf{R}} + \epsilon_5 \mathbf{I}_N,$$

we have a distributionally robust beamformer

$$\mathbf{W}_{\text{DR-R}}^* = \mathbf{P} \mathbf{H}^H [\mathbf{H} \mathbf{P} \mathbf{H}^H + \hat{\mathbf{R}} + \epsilon_5 \mathbf{I}_N]^{-1}, \quad (32)$$

which is also a diagonally loaded beamformer.  $\square$

*Example 5 (Generalized Diagonal Loading):* The generalized diagonally loaded beamformer can be obtained if  $\mathbf{R}_x \preceq \hat{\mathbf{R}}_x + \epsilon \mathbf{F}$  or  $\mathbf{R} \preceq \hat{\mathbf{R}} + \epsilon \mathbf{F}$  for some  $\mathbf{F} \succeq \mathbf{0}$ :

$$\begin{aligned} \mathbf{W}_{\text{DR-GDL}}^* &= \mathbf{R}_{xs}^H [\hat{\mathbf{R}}_x + \epsilon \mathbf{F}]^{-1} \\ &= \mathbf{P} \mathbf{H}^H [\mathbf{H} \mathbf{P} \mathbf{H}^H + \hat{\mathbf{R}} + \epsilon \mathbf{F}]^{-1}. \end{aligned} \quad (33)$$

When  $\mathbf{H}$  is known, we can choose  $\mathbf{F} := \mathbf{H} \mathbf{H}^H$ , which is reminiscent of (31).  $\square$

From Examples 1-5, we can see that the popular diagonally loaded beamformer (27) and the proposed generalized diagonally loaded beamformer (33) can combat several types of uncertainties including the limited training sample size, the uncertainty in the covariance of the transmitted signal, the uncertainty in the covariance of the channel noise, etc. However, the uncertainty sets are quite specially constructed, e.g., using the diagonal  $\epsilon$ -perturbation method, the eigenvalue thresholding method, or the  $\mathbf{F}$  matrix.

In addition, Example 2 motivates the following important theorem, which justifies the popular ridge regression in machine learning.

*Theorem 2 (Ridge Regression and Tikhonov Regularization):* Consider a linear regression problem

$$\mathbf{s} = \mathbf{W} \mathbf{x} + \mathbf{e},$$

and the distributionally robust linear estimator of  $\mathbf{W}$

$$\min_{\mathbf{W} \in \mathbb{C}^{M \times N}} \max_{\mathbb{P}_{\mathbf{x}, \mathbf{s}} \in \mathcal{U}_{\mathbf{x}, \mathbf{s}}} \text{Tr} \mathbb{E}_{\mathbf{x}, \mathbf{s}} [\mathbf{W} \mathbf{x} - \mathbf{s}] [\mathbf{W} \mathbf{x} - \mathbf{s}]^H,$$

which can be particularized to (19). Supposing that the second-order moment of  $\mathbf{x}$  is uncertain and quantified as

$$\hat{\mathbf{R}}_x - \epsilon_1 \mathbf{I}_N \preceq \mathbf{R}_x \preceq \hat{\mathbf{R}}_x + \epsilon_1 \mathbf{I}_N,$$

<sup>1</sup>This claim can be routinely proven in analogy to Theorem 1 and a real-space case in [29, Thm. 1].

then the distributionally robust linear estimator of  $\mathbf{W}$  becomes a ridge regression (i.e., squared- $F$ -norm regularized) method

$$\min_{\mathbf{W}} \text{Tr} [\mathbf{W} \hat{\mathbf{R}}_x \mathbf{W}^H - \mathbf{W} \hat{\mathbf{R}}_{xs} - \hat{\mathbf{R}}_{xs}^H \mathbf{W}^H + \hat{\mathbf{R}}_s] + \epsilon \text{Tr} [\mathbf{W} \mathbf{W}^H].$$

The regularization term becomes  $\text{Tr} [\mathbf{W} \mathbf{W}^H]$ , which is known as the Tikhonov regularizer, if

$$\hat{\mathbf{R}}_x - \epsilon \mathbf{F} \preceq \mathbf{R}_x \preceq \hat{\mathbf{R}}_x + \epsilon \mathbf{F}$$

is employed for some  $\mathbf{F} \succeq \mathbf{0}$ .

*Proof:* This is due to Lemma 1 and Theorem 1. Just note that  $\text{Tr} [\mathbf{W} (\hat{\mathbf{R}}_x + \epsilon \mathbf{F}) \mathbf{W}^H - \mathbf{W} \hat{\mathbf{R}}_{xs} - \hat{\mathbf{R}}_{xs}^H \mathbf{W}^H + \hat{\mathbf{R}}_s] = \text{Tr} [\mathbf{W} \hat{\mathbf{R}}_x \mathbf{W}^H - \mathbf{W} \hat{\mathbf{R}}_{xs} - \hat{\mathbf{R}}_{xs}^H \mathbf{W}^H + \hat{\mathbf{R}}_s] + \epsilon \text{Tr} [\mathbf{W} \mathbf{W}^H]$ . This completes the proof.  $\square$

Note that in Theorem 2, the second-order moment of  $\mathbf{s}$  is not considered because it does not influence the optimal solution of  $\mathbf{W}$ : i.e., the optimal solution of  $\mathbf{W}$  does not depend on the value of  $\mathbf{R}_s$ . Theorem 2 gives a theoretical interpretation of the popular ridge regression in machine learning from the perspective of distributional robustness.<sup>2</sup> When the uncertainty is quantified by the Wasserstein distance, a similar result can be seen in [30, Prop. 3], which however is not a ridge regression formulation because in [30, Prop. 3], the loss function is square-rooted and the norm regularizer is not squared; cf. also [27, Rem. 18 and 19]. The corollary below justifies the rationale of any norm-regularized method.

*Corollary 1:* The following squared-norm-regularized beamforming formulation can combat the distributional uncertainty:

$$\min_{\mathbf{W}} \text{Tr} [\mathbf{W} \hat{\mathbf{R}}_x \mathbf{W}^H - \mathbf{W} \hat{\mathbf{R}}_{xs} - \hat{\mathbf{R}}_{xs}^H \mathbf{W}^H + \hat{\mathbf{R}}_s] + \lambda \|\mathbf{W}\|^2, \quad (34)$$

where  $\|\cdot\|$  denotes any matrix norm. This is because all norms on  $\mathbb{C}^{M \times N}$  are equivalent; hence, there exists some  $\lambda \geq 0$  such that  $\lambda \|\mathbf{W}\|^2 \geq \epsilon \|\mathbf{W}\|_F^2 = \epsilon \text{Tr} [\mathbf{W} \mathbf{W}^H]$ . As a result, (34) can upper bound the ridge cost in Theorem 2.  $\square$

Motivated by Theorem 2, the following corollary is immediate, which gives another interpretation of ridge regression and Tikhonov regularization from the perspective of data augmentation through data perturbation (i.e., the noise injection method in machine learning).

*Corollary 2 (Data Augmentation for Linear Regression):* Consider a linear regression problem on  $(\mathbf{x}, \mathbf{s})$  with data perturbation vectors  $(\Delta_x, \Delta_s)$

$$(\mathbf{s} + \Delta_s) = \mathbf{W}(\mathbf{x} + \Delta_x) + \mathbf{e},$$

and the distributionally robust linear estimator of  $\mathbf{W}$

$$\min_{\mathbf{W} \in \mathbb{C}^{M \times N}} \max_{\mathbb{P}_{\Delta_x, \Delta_s} \in \mathcal{U}_{\Delta_x, \Delta_s}} \text{Tr} \mathbb{E}_{(\mathbf{x}, \mathbf{s}) \sim \hat{\mathbb{P}}_{\mathbf{x}, \mathbf{s}}} \mathbb{E}_{\Delta_x, \Delta_s} \left\{ [\mathbf{W}(\mathbf{x} + \Delta_x) - (\mathbf{s} + \Delta_s)][\mathbf{W}(\mathbf{x} + \Delta_x) - (\mathbf{s} + \Delta_s)]^H \right\}.$$

Suppose that  $\Delta_x$  is uncorrelated with  $\mathbf{x}$ , with  $\mathbf{s}$ , and with  $\Delta_s$ ; in addition,  $\Delta_s$  is uncorrelated with  $\mathbf{x}$ . If the second-order moment of  $\Delta_x$  is upper bounded as  $\mathbb{E} \Delta_x \Delta_x^H \preceq \epsilon \mathbf{I}_N$ , then the distributionally robust linear estimator of  $\mathbf{W}$  becomes a ridge regression (i.e., squared- $F$ -norm regularized) method

$$\min_{\mathbf{W}} \text{Tr} [\mathbf{W} \hat{\mathbf{R}}_x \mathbf{W}^H - \mathbf{W} \hat{\mathbf{R}}_{xs} - \hat{\mathbf{R}}_{xs}^H \mathbf{W}^H + \hat{\mathbf{R}}_s] + \epsilon \text{Tr} [\mathbf{W} \mathbf{W}^H].$$

<sup>2</sup>This is the first time to provide the ridge regression with an interpretation of distributional robustness.

The regularization term becomes  $\text{Tr} [\mathbf{W} \mathbf{W}^H]$ , which is known as the Tikhonov regularizer, if  $\mathbb{E} \Delta_x \Delta_x^H \preceq \epsilon \mathbf{F}$ , for some  $\mathbf{F} \succeq \mathbf{0}$ .  $\square$

The second-order moment of  $\Delta_s$  is not considered in Corollary 2 as it does not influence the optimal value of  $\mathbf{W}$ .

### B. Non-Trivial Uncertainty Sets

Below we study more general and non-trivial construction methods for the uncertainty sets of  $\mathbf{R}_x$ ,  $\mathbf{P}$ , and  $\mathbf{R}$  using the Wasserstein distance and the  $F$ -norm, beyond the simple diagonal  $\epsilon$ -perturbation method and the eigenvalue thresholding method.

1) *Wasserstein Distributionally Robust Beamforming:* We start with the case of  $\mathbf{R}_x$ :

$$\begin{aligned} \max_{\mathbf{R}_x} \quad & \text{Tr} [-\mathbf{R}_{xs}^H \mathbf{R}_x^{-1} \mathbf{R}_{xs} + \mathbf{R}_s] \\ \text{s.t.} \quad & \text{Tr} [\mathbf{R}_x + \hat{\mathbf{R}}_x - 2(\hat{\mathbf{R}}_x^{1/2} \mathbf{R}_x \hat{\mathbf{R}}_x^{1/2})^{1/2}] \leq \epsilon_1^2 \\ & \mathbf{R}_x \succeq \mathbf{0}, \mathbf{R}_x = \mathbf{R}_x^H, \end{aligned} \quad (35)$$

where we assumed that the pseudo-covariance (i.e., relation matrix) of the complex vector  $\mathbf{x}$  has not been perturbed. Otherwise, supposing the pseudo-covariance of  $\mathbf{x}$  is  $\mathbf{C}_x$ , we can consider one more constraint

$$\text{Tr} [\mathbf{C}_x + \hat{\mathbf{C}}_x - 2(\hat{\mathbf{C}}_x^{1/2} \mathbf{C}_x \hat{\mathbf{C}}_x^{1/2})^{1/2}] \leq \epsilon_{1,2}^2,$$

where  $\epsilon_{1,2} \geq 0$  is an uncertainty quantification parameter for the uncertainty in  $\hat{\mathbf{C}}_x$ .

Problem (35) is a nonlinear positive semi-definite program (P-SDP). However, we can give it a linear reformulation.

*Proposition 1:* Problem (35) is equivalent to a linear P-SDP

$$\begin{aligned} \max_{\mathbf{R}_x, \mathbf{V}, \mathbf{U}} \quad & \text{Tr} [-\mathbf{V} + \mathbf{R}_s] \\ \text{s.t.} \quad & \begin{bmatrix} \mathbf{V} & \mathbf{R}_{xs}^H \\ \mathbf{R}_{xs} & \mathbf{R}_x \end{bmatrix} \succeq \mathbf{0} \\ & \text{Tr} [\mathbf{R}_x + \hat{\mathbf{R}}_x - 2\mathbf{U}] \leq \epsilon_1^2 \\ & \begin{bmatrix} \hat{\mathbf{R}}_x^{1/2} \mathbf{R}_x \hat{\mathbf{R}}_x^{1/2} & \mathbf{U} \\ \mathbf{U} & \mathbf{I}_N \end{bmatrix} \succeq \mathbf{0} \\ & \mathbf{R}_x = \mathbf{R}_x^H, \mathbf{V} = \mathbf{V}^H, \mathbf{U} = \mathbf{U}^H \\ & \mathbf{R}_x \succeq \mathbf{0}, \mathbf{V} \succeq \mathbf{0}, \mathbf{U} \succeq \mathbf{0}. \end{aligned} \quad (36)$$

*Proof:* See Appendix F of the online supplementary materials.  $\square$

Complex-valued linear P-SDP can be solved using the YALMIP solver.<sup>3</sup>

Suppose that  $\mathbf{R}_x^*$  solves (36). The corresponding Wasserstein distributionally robust beamformer is given as

$$\mathbf{W}_{\text{DR-Wasserstein}}^* = \mathbf{R}_{xs}^H \mathbf{R}_x^{*-1}. \quad (37)$$

Next, we investigate the case of uncertain  $\hat{\mathbf{P}}$  and  $\hat{\mathbf{R}}$ . From (24), we have

$$\begin{aligned} \max_{\mathbf{P}, \mathbf{R}} \quad & \text{Tr} [\mathbf{P} - \mathbf{P} \mathbf{H}^H (\mathbf{H} \mathbf{P} \mathbf{H}^H + \mathbf{R})^{-1} \mathbf{H} \mathbf{P}] \\ \text{s.t.} \quad & \text{Tr} [\mathbf{P} + \hat{\mathbf{P}} - 2(\hat{\mathbf{P}}^{1/2} \mathbf{P} \hat{\mathbf{P}}^{1/2})^{1/2}] \leq \epsilon_4^2 \\ & \text{Tr} [\mathbf{R} + \hat{\mathbf{R}} - 2(\hat{\mathbf{R}}^{1/2} \mathbf{R} \hat{\mathbf{R}}^{1/2})^{1/2}] \leq \epsilon_5^2 \\ & \mathbf{P} = \mathbf{P}^H, \mathbf{R} = \mathbf{R}^H \\ & \mathbf{P} \succeq \mathbf{0}, \mathbf{R} \succeq \mathbf{0}, \end{aligned} \quad (38)$$

<sup>3</sup>See <https://yalmip.github.io/inside/complexproblems/>.

where we have assumed that the pseudo-covariances of the complex vectors  $\mathbf{s}$  and  $\mathbf{v}$  have not been perturbed.

Problem (38) can be transformed into a linear P-SDP using a similar technique in the proof of Proposition 1. One can just introduce an inequality  $\mathbf{U} \succeq \mathbf{P}\mathbf{H}^H(\mathbf{H}\mathbf{P}\mathbf{H}^H + \mathbf{R})^{-1}\mathbf{H}\mathbf{P}$  and the objective function will become  $\text{Tr}[\mathbf{P} - \mathbf{U}]$ .

Suppose that  $(\mathbf{P}^*, \mathbf{R}^*)$  solves (38). The corresponding Wasserstein distributionally robust beamformer is given as

$$\mathbf{W}_{\text{DR-Wasserstein-PR}}^* = \mathbf{P}^*\mathbf{H}^H[\mathbf{H}\mathbf{P}^*\mathbf{H}^H + \mathbf{R}^*]^{-1}. \quad (39)$$

The Wasserstein distance is valid for Hermitian positive semi-definite matrices that are covariance matrices of Gaussian distributions. Therefore, we cannot use the Wasserstein distance to measure the differences between  $\mathbf{R}_{xs}$  and  $\hat{\mathbf{R}}_{xs}$ , and between  $\mathbf{H}$  and  $\hat{\mathbf{H}}$ . In this case, the  $F$ -norm of matrices can be used.

2) *F-Norm Distributionally Robust Beamforming*: Under the  $F$ -norm, we just need to replace the Wasserstein distance. To be specific, for example, (35) becomes

$$\begin{aligned} \max_{\mathbf{R}_x} \quad & \text{Tr}[-\mathbf{R}_{xs}^H \mathbf{R}_x^{-1} \mathbf{R}_{xs} + \mathbf{R}_s] \\ \text{s.t.} \quad & \text{Tr}[(\mathbf{R}_x - \hat{\mathbf{R}}_x)^H (\mathbf{R}_x - \hat{\mathbf{R}}_x)] \leq \epsilon_1^2 \\ & \mathbf{R}_x \succeq \mathbf{0}, \quad \mathbf{R}_x = \mathbf{R}_x^H, \end{aligned} \quad (40)$$

The linear reformulation of the above display is given in the proposition below.

*Proposition 2*: The nonlinear P-SDP (40) can be equivalently reformulated into a linear P-SDP

$$\begin{aligned} \max_{\mathbf{R}_x, \mathbf{V}, \mathbf{U}} \quad & \text{Tr}[-\mathbf{V} + \mathbf{R}_s] \\ \text{s.t.} \quad & \begin{bmatrix} \mathbf{V} & \mathbf{R}_{xs}^H \\ \mathbf{R}_{xs} & \mathbf{R}_x \end{bmatrix} \succeq \mathbf{0} \\ & \text{Tr}[\mathbf{U}] \leq \epsilon_1^2, \\ & \begin{bmatrix} \mathbf{U} & (\mathbf{R}_x - \hat{\mathbf{R}}_x)^H \\ (\mathbf{R}_x - \hat{\mathbf{R}}_x) & \mathbf{I}_N \end{bmatrix} \succeq \mathbf{0}, \\ & \mathbf{R}_x = \mathbf{R}_x^H, \quad \mathbf{V} = \mathbf{V}^H, \quad \mathbf{U} = \mathbf{U}^H \\ & \mathbf{R}_x \succeq \mathbf{0}, \quad \mathbf{V} \succeq \mathbf{0}, \quad \mathbf{U} \succeq \mathbf{0}. \end{aligned} \quad (41)$$

*Proof*: This is by applying the Schur complement.  $\square$

As for the maximization over  $\mathbf{R}_{xs}$  that cannot be characterized using the Wasserstein distance, we have

$$\begin{aligned} \max_{\mathbf{R}_{xs}} \quad & \text{Tr}[-\mathbf{R}_{xs}^H \mathbf{R}_x^{-1} \mathbf{R}_{xs} + \mathbf{R}_s] \\ \text{s.t.} \quad & \text{Tr}[(\mathbf{R}_{xs} - \hat{\mathbf{R}}_{xs})^H (\mathbf{R}_{xs} - \hat{\mathbf{R}}_{xs})] \leq \epsilon_2^2, \end{aligned} \quad (42)$$

which can be solved using, e.g., the projected gradient descent method, because it is a convex program. Note that the gradient of the objective function with respect to  $\mathbf{R}_{xs}$  is  $-2\mathbf{R}_x^{-1}\mathbf{R}_{xs}$ .

### C. Multi-Frame Case: Dynamic Channel Evolution

Each frame contains a pilot block used for beamformer design. Although the channel state information (CSI) may change from one frame to another, the CSI between the two consecutive frames is highly correlated. This correlation can benefit beamformer design across multiple frames. Suppose that  $\{(s_1, \mathbf{x}_1), (s_2, \mathbf{x}_2), \dots, (s_L, \mathbf{x}_L)\}$  is the training data in the current frame and  $\{(s'_1, \mathbf{x}'_1), (s'_2, \mathbf{x}'_2), \dots, (s'_L, \mathbf{x}'_L)\}$  is the history data in the immediately preceding frame. In

such a case, the distributional difference between  $\hat{\mathbb{P}}_{\mathbf{x}, \mathbf{s}}$  and  $\hat{\mathbb{P}}_{\mathbf{x}', \mathbf{s}'}$  is upper bounded, that is,  $d(\hat{\mathbb{P}}_{\mathbf{x}, \mathbf{s}}, \hat{\mathbb{P}}_{\mathbf{x}', \mathbf{s}'}) \leq \epsilon'$  for some proper distance  $d$  and a real number  $\epsilon' \geq 0$  where  $\hat{\mathbb{P}}_{\mathbf{x}, \mathbf{s}} := \frac{1}{L} \sum_{i=1}^L \delta_{(\mathbf{x}_i, \mathbf{s}_i)}$  and  $\hat{\mathbb{P}}_{\mathbf{x}', \mathbf{s}'} := \frac{1}{L} \sum_{i=1}^L \delta_{(\mathbf{x}'_i, \mathbf{s}'_i)}$ .

Since a beamformer  $\mathbf{W} = \mathcal{F}(\mathbb{P}_{\mathbf{x}, \mathbf{s}})$  is a continuous functional  $\mathcal{F}(\cdot)$  of data distribution  $\mathbb{P}_{\mathbf{x}, \mathbf{s}}$ , cf. (11), we have  $\|\mathbf{W} - \mathbf{W}'\|_F = \|\mathcal{F}(\hat{\mathbb{P}}_{\mathbf{x}, \mathbf{s}}) - \mathcal{F}(\hat{\mathbb{P}}_{\mathbf{x}', \mathbf{s}'})\|_F \leq C \cdot d(\hat{\mathbb{P}}_{\mathbf{x}, \mathbf{s}}, \hat{\mathbb{P}}_{\mathbf{x}', \mathbf{s}'}) \leq \epsilon$  for some positive constant  $C \geq 0$  and upper bound  $\epsilon \geq 0$  where  $\mathbf{W}'$  is the beamformer associated with  $\hat{\mathbb{P}}_{\mathbf{x}', \mathbf{s}'}$  in the previous frame. Therefore, the beamforming problem (12) becomes a constrained problem

$$\begin{aligned} \min_{\mathbf{W}} \quad & \text{Tr}[\mathbf{W}\mathbf{R}_x\mathbf{W}^H - \mathbf{W}\mathbf{R}_{xs} - \mathbf{R}_{xs}^H\mathbf{W}^H + \mathbf{R}_s] \\ \text{s.t.} \quad & \text{Tr}[\mathbf{W} - \mathbf{W}'][\mathbf{W} - \mathbf{W}']^H \leq \epsilon^2. \end{aligned}$$

By the Lagrange duality theory, it is equivalent to

$$\begin{aligned} \min_{\mathbf{W}} \quad & \text{Tr}[\mathbf{W}\mathbf{R}_x\mathbf{W}^H - \mathbf{W}\mathbf{R}_{xs} - \mathbf{R}_{xs}^H\mathbf{W}^H + \mathbf{R}_s] + \\ & \lambda \cdot \text{Tr}[\mathbf{W} - \mathbf{W}'][\mathbf{W} - \mathbf{W}']^H \\ = \min_{\mathbf{W}} \quad & \text{Tr}[\mathbf{W}(\mathbf{R}_x + \lambda\mathbf{I}_N)\mathbf{W}^H - \mathbf{W}(\mathbf{R}_{xs} + \lambda\mathbf{W}^H) - \\ & (\mathbf{R}_{xs} + \lambda\mathbf{W}^H)^H\mathbf{W}^H + (\mathbf{R}_s + \lambda\mathbf{W}'\mathbf{W}^H)], \end{aligned} \quad (43)$$

for some  $\lambda \geq 0$ . As a result, we have the Wiener beamformer for the multi-frame case, where we can treat  $\mathbf{W}'$  as a *prior knowledge* of  $\mathbf{W}$ .

*Claim 1 (Multi-Frame Beamforming)*: The Wiener beamformer for the multi-frame case is given by

$$\begin{aligned} \mathbf{W}_{\text{Wiener-MF}}^* &= [\mathbf{R}_{xs} + \lambda\mathbf{W}^H][\mathbf{R}_x + \lambda\mathbf{I}_N]^{-1} \\ &= [\mathbf{P}\mathbf{H}^H + \lambda\mathbf{W}^H][\mathbf{H}\mathbf{P}\mathbf{H}^H + \mathbf{R} + \lambda\mathbf{I}_N]^{-1}, \end{aligned} \quad (44)$$

where  $\lambda \geq 0$  is a tuning parameter to control the similarity between  $\mathbf{W}$  and  $\mathbf{W}'$ . Specifically, if  $\lambda$  is large,  $\mathbf{W}$  must be close to  $\mathbf{W}'$ ; if  $\lambda$  is small,  $\mathbf{W}$  can be far away from  $\mathbf{W}'$ .  $\square$

With the result in Claim 1, (22) becomes

$$\begin{aligned} \max_{\mathbf{R}_x, \mathbf{R}_{xs}, \mathbf{R}_s} \quad & \text{Tr}[-(\mathbf{R}_{xs} + \lambda\mathbf{W}^H)^H \cdot (\mathbf{R}_x + \lambda\mathbf{I}_N)^{-1} \cdot \\ & (\mathbf{R}_{xs} + \lambda\mathbf{W}^H) + (\mathbf{R}_s + \lambda\mathbf{W}'\mathbf{W}^H)] \\ \text{s.t.} \quad & d_1(\mathbf{R}_x, \hat{\mathbf{R}}_x) \leq \epsilon_1, \\ & d_2(\mathbf{R}_{xs}, \hat{\mathbf{R}}_{xs}) \leq \epsilon_2, \\ & d_3(\mathbf{R}_s, \hat{\mathbf{R}}_s) \leq \epsilon_3, \\ & \mathbf{R}_x \succeq \mathbf{0}, \quad \mathbf{R}_x = \mathbf{R}_x^H, \\ & \mathbf{R}_s \succeq \mathbf{0}, \quad \mathbf{R}_s = \mathbf{R}_s^H, \end{aligned} \quad (45)$$

whose objective function is monotonically increasing in  $\mathbf{R}_x$  and  $\mathbf{R}_s$ .

The remaining distributional robustness modeling and analyses against the uncertainties in  $\mathbf{R}_x$ ,  $\mathbf{R}_{xs}$ ,  $\mathbf{P}$ , and  $\mathbf{R}$  are technically straightforward, and therefore, we omit them here. Upon using the diagonal loading method on  $\hat{\mathbf{R}}_x$ , a distributionally robust beamformer for the multi-frame case is

$$\mathbf{W}_{\text{DR-Wiener-MF}}^* = [\mathbf{P}\mathbf{H}^H + \lambda\mathbf{W}^H] \cdot [\mathbf{H}\mathbf{P}\mathbf{H}^H + \mathbf{R} + \lambda\mathbf{I}_N + \epsilon_1\mathbf{I}_N]^{-1},$$

where  $\epsilon_1$  is an uncertainty quantification parameter for  $\hat{\mathbf{R}}_x$ .

### V. DISTRIBUTIONALLY ROBUST NONLINEAR ESTIMATION

For the convenience of the technical treatment, we study the estimation problem in real spaces. Nonlinear estimators

are to be limited in reproducing kernel Hilbert spaces and feedforward multi-layer neural network function spaces.

### A. Reproducing Kernel Hilbert Spaces

1) *General Framework and Concrete Examples:* As a standard treatment in machine learning, we use the partial pilot data  $\{\underline{x}_1, \underline{x}_2, \dots, \underline{x}_L\}$  to construct the reproducing kernel Hilbert spaces, and use the whole pilot data  $\{(\underline{x}_1, \underline{s}_1), (\underline{x}_2, \underline{s}_2), \dots, (\underline{x}_L, \underline{s}_L)\}$  to train the optimal estimator in an RKHS.

With the  $\mathbf{W}$ -linear representation of  $\phi(\cdot)$  in (2), i.e.,  $\phi(\cdot) = \mathbf{W}\varphi(\cdot)$ , the distributionally robust estimation problem (17) becomes

$$\min_{\mathbf{W} \in \mathbb{R}^{2M \times L}} \max_{\mathbb{P}_{\underline{x}, \underline{s}} \in \mathcal{U}_{\underline{x}, \underline{s}}} \text{Tr} \mathbb{E}_{\underline{x}, \underline{s}} [\mathbf{W} \cdot \varphi(\underline{x}) - \underline{s}] [\mathbf{W} \cdot \varphi(\underline{x}) - \underline{s}]^\top, \quad (46)$$

which is linear in  $\mathbf{W}$ . The proposition below gives the reformulation and solution of (46).

*Proposition 3:* Let  $\mathbf{K}$  denote the *kernel matrix* associated with the kernel function  $\ker(\cdot, \cdot)$  whose  $(i, j)$ -entry is defined as

$$\mathbf{K}_{i,j} := \ker(\underline{x}_i, \underline{x}_j), \quad \forall i, j \in [L].$$

Then, the distributionally robust  $\underline{x}$ -nonlinear estimation problem (46) can be rewritten as a distributionally robust beamforming problem as

$$\begin{aligned} \min_{\mathbf{W}} \max_{\mathbf{R}_z, \mathbf{R}_{zs}, \mathbf{R}_s} \quad & \text{Tr} [\mathbf{W} \mathbf{R}_z \mathbf{W}^\top - \mathbf{W} \mathbf{R}_{zs} - \mathbf{R}_{zs}^\top \mathbf{W}^\top + \mathbf{R}_s] \\ \text{s.t.} \quad & d_1(\mathbf{R}_z, \hat{\mathbf{R}}_z) \leq \epsilon_1, \\ & d_2(\mathbf{R}_{zs}, \hat{\mathbf{R}}_{zs}) \leq \epsilon_2, \\ & d_3(\mathbf{R}_s, \hat{\mathbf{R}}_s) \leq \epsilon_3, \\ & \mathbf{R}_z \succeq 0, \quad \mathbf{R}_z = \mathbf{R}_z^\top, \\ & \mathbf{R}_s \succeq 0, \quad \mathbf{R}_s = \mathbf{R}_s^\top, \end{aligned} \quad (47)$$

where  $\hat{\mathbf{R}}_z := \frac{1}{L} \mathbf{K}^2$ ,  $\hat{\mathbf{R}}_{zs} := \frac{1}{L} \mathbf{K} \mathbf{S}^\top$ ,  $\hat{\mathbf{R}}_s := \frac{1}{L} \mathbf{S} \mathbf{S}^\top$ , and  $\underline{\mathbf{S}} := [\text{Re } \mathbf{S}; \text{Im } \mathbf{S}] = [\underline{s}_1, \underline{s}_2, \dots, \underline{s}_L]$ . In addition, the strong min-max property holds for (47): i.e., the order of min and max can be exchanged provided that the first three constraints are convex. As a result, given every pair of  $(\mathbf{R}_z, \mathbf{R}_{zs}, \mathbf{R}_s)$ , the optimal Wiener beamformer is<sup>4</sup>

$$\mathbf{W}_{\text{RKHS}}^* = \hat{\mathbf{R}}_{zs}^\top \hat{\mathbf{R}}_z^{-1} = \underline{\mathbf{S}} \mathbf{K} \mathbf{K}^{-2} = \underline{\mathbf{S}} \mathbf{K}^{-1}, \quad (48)$$

which transforms (47) to

$$\begin{aligned} \max_{\mathbf{R}_z, \mathbf{R}_{zs}, \mathbf{R}_s} \quad & \text{Tr} [-\mathbf{R}_{zs}^\top \mathbf{R}_z^{-1} \mathbf{R}_{zs} + \mathbf{R}_s] \\ \text{s.t.} \quad & d_1(\mathbf{R}_z, \hat{\mathbf{R}}_z) \leq \epsilon_1, \\ & d_2(\mathbf{R}_{zs}, \hat{\mathbf{R}}_{zs}) \leq \epsilon_2, \\ & d_3(\mathbf{R}_s, \hat{\mathbf{R}}_s) \leq \epsilon_3, \\ & \mathbf{R}_z \succeq 0, \quad \mathbf{R}_z = \mathbf{R}_z^\top, \\ & \mathbf{R}_s \succeq 0, \quad \mathbf{R}_s = \mathbf{R}_s^\top. \end{aligned} \quad (49)$$

*Proof:* The key is to treat  $\varphi(\underline{x})$  as a new random vector  $\underline{z} \in \mathbb{R}^L$ . For details, see Appendix G of the online supplementary materials.  $\square$

In (47),  $d_1$ ,  $d_2$ , and  $d_3$  define three matrix similarity measures to quantify the uncertainties in  $\hat{\mathbf{R}}_z$ ,  $\hat{\mathbf{R}}_{zs}$ , and  $\hat{\mathbf{R}}_s$ ,

<sup>4</sup>For numerical stability in the inversion of  $\mathbf{K}$ ,  $L$  should not be too large.

respectively;  $\epsilon_1 \geq 0$ ,  $\epsilon_2 \geq 0$ , and  $\epsilon_3 \geq 0$  quantify the uncertainty levels. Proposition 3 reveals the benefit of the kernel trick (2), that is, the possibility to represent a nonlinear estimation problem as a linear one.

The claim below summarizes the solution of (17) in the RKHS induced by the kernel function  $\ker(\cdot, \cdot)$ .

*Claim 2:* Suppose that  $(\mathbf{R}_z^*, \mathbf{R}_{zs}^*, \mathbf{R}_s^*)$  solves (49). Then the optimal estimator of (17) in the RKHS induced by  $\ker(\cdot, \cdot)$  is given by

$$\phi^*(\underline{x}) = \mathbf{\Gamma}_M \cdot \mathbf{R}_{zs}^{*\top} \cdot \mathbf{R}_z^{*-1} \cdot \varphi(\underline{x}), \quad (50)$$

where  $\underline{x} = [\text{Re } \underline{x}; \text{Im } \underline{x}]$  is the real-space representation of  $\underline{x}$ ,  $\mathbf{\Gamma}_M := [\mathbf{I}_M, \mathbf{J}_M]$  is defined in Subsection I-B, and

$$\varphi(\underline{x}) := \begin{bmatrix} \ker(\underline{x}, \underline{x}_1) \\ \ker(\underline{x}, \underline{x}_2) \\ \vdots \\ \ker(\underline{x}, \underline{x}_L) \end{bmatrix}.$$

In addition, the corresponding worst-case estimation error covariance is

$$\mathbf{\Gamma}_M \cdot [-\mathbf{R}_{zs}^{*\top} \mathbf{R}_z^{*-1} \mathbf{R}_{zs}^* + \mathbf{R}_s^*] \cdot \mathbf{\Gamma}_M^\top, \quad (51)$$

which upper bounds the true estimation error covariance.  $\square$

Concrete examples of Claim 2 are given as follows.

*Example 6 (Kernelized Diagonal Loading):* By using

$$\hat{\mathbf{R}}_z - \epsilon_1 \mathbf{I}_L \preceq \mathbf{R}_z \preceq \hat{\mathbf{R}}_z + \epsilon_1 \mathbf{I}_L,$$

we have the kernelized diagonal loading method

$$\phi^*(\underline{x}) = \mathbf{\Gamma}_M \cdot \frac{1}{L} \underline{\mathbf{S}} \mathbf{K} \cdot \left( \frac{1}{L} \mathbf{K}^2 + \epsilon_1 \mathbf{I}_L \right)^{-1} \cdot \varphi(\underline{x}), \quad (52)$$

which is obtained at the upper bound of  $\mathbf{R}_z$ . Furthermore, in this case, the distributionally robust formulation (46) is equivalent to a squared- $F$ -norm-regularized formulation

$$\begin{aligned} \min_{\mathbf{W} \in \mathbb{R}^{2M \times L}} \quad & \text{Tr} \mathbb{E}_{\underline{x}, \underline{s}} [\mathbf{W} \cdot \varphi(\underline{x}) - \underline{s}] [\mathbf{W} \cdot \varphi(\underline{x}) - \underline{s}]^\top + \\ & \epsilon_1 \cdot \text{Tr} [\mathbf{W} \mathbf{W}^\top], \end{aligned} \quad (53)$$

which can be proven by replacing  $\mathbf{R}_z$  in (47) with its upper bound.  $\square$

*Example 7 (Kernelized Eigenvalue Thresholding):* The kernelized eigenvalue thresholding method can be designed in analogy to Example 3. The two key steps are to obtain the eigenvalue decomposition of  $\hat{\mathbf{R}}_z = \mathbf{K}^2/L$  and then lift the eigenvalues; cf. (29).  $\square$

In addition, Example 6 motivates the following important theorem for statistical machine learning.

*Theorem 3 (Kernel Ridge Regression and Kernel Tikhonov Regularization):* Consider the nonlinear regression problem

$$\mathbf{s} = \phi(\underline{x}) + \mathbf{e},$$

and the distributionally robust estimator of  $\phi(\underline{x}) = \mathbf{W} \cdot \varphi(\underline{x})$  in the RKHS induced by the kernel function  $\ker(\cdot, \cdot)$ , i.e.,

$$\min_{\mathbf{W} \in \mathbb{R}^{2M \times L}} \max_{\mathbb{P}_{\underline{x}, \underline{s}} \in \mathcal{U}_{\underline{x}, \underline{s}}} \text{Tr} \mathbb{E}_{\underline{x}, \underline{s}} [\mathbf{W} \cdot \varphi(\underline{x}) - \underline{s}] [\mathbf{W} \cdot \varphi(\underline{x}) - \underline{s}]^\top.$$

Supposing that only the second-order moment of  $\underline{z} := \varphi(\underline{x})$  is uncertain and quantified as

$$\hat{\mathbf{R}}_z - \epsilon \mathbf{I}_L \preceq \mathbf{R}_z \preceq \hat{\mathbf{R}}_z + \epsilon \mathbf{I}_L,$$

then the distributionally robust estimator of  $\mathbf{W}$  becomes a kernel ridge regression method (53). The regularization term in (53) becomes the Tikhonov regularizer  $\text{Tr}[\mathbf{W}\mathbf{F}\mathbf{W}^\top]$  if

$$\hat{\mathbf{R}}_{\underline{z}} - \epsilon\mathbf{F} \preceq \mathbf{R}_{\underline{z}} \preceq \hat{\mathbf{R}}_{\underline{z}} + \epsilon\mathbf{F}$$

is employed for some  $\mathbf{F} \succeq \mathbf{0}$ .

*Proof:* See Example 6; cf. Theorem 2.  $\square$

This is the first time to give the kernel ridge regression an interpretation of distributional robustness. The usual choice of  $\mathbf{F}$  in Theorem 3 is the  $L$ -divided kernel matrix  $\mathbf{K}/L$ ; see, e.g., [31, Eq. (4)], [24, Eqs. (15.110) and (15.113)]. As a result, from (52), we have

$$\phi^*(\mathbf{x}) = \Gamma_M \cdot \underline{\mathbf{S}} \cdot (\mathbf{K} + \epsilon_1 \mathbf{I}_L)^{-1} \cdot \varphi(\mathbf{x}), \quad (54)$$

which is another type of kernel ridge regression (i.e., a new kernelized diagonal loading method).

In analogy to Corollary 1, the following corollary motivated from (53) is immediate.

*Corollary 3:* The following squared-norm-regularized method in RKHSs can combat the distributional uncertainty:

$$\min_{\mathbf{W} \in \mathbb{R}^{2M \times L}} \text{Tr} \mathbb{E}_{\underline{\mathbf{x}}, \underline{\mathbf{s}}} [\mathbf{W} \cdot \varphi(\mathbf{x}) - \underline{\mathbf{s}}] [\mathbf{W} \cdot \varphi(\mathbf{x}) - \underline{\mathbf{s}}]^\top + \lambda \cdot \|\mathbf{W}\|^2, \quad (55)$$

for any matrix norm  $\|\cdot\|$ ; cf. Corollary 1.  $\square$

Moreover, in analogy to Corollary 2, the following corollary is immediate.

*Corollary 4 (Data Augmentation for Kernel Regression):* Consider the nonlinear regression problem in Theorem 3. Its data-perturbed counterpart can be constructed by taking into account the data perturbation vectors  $(\Delta_{\underline{s}}, \Delta_{\underline{z}})$ . Suppose that  $\Delta_{\underline{z}}$  is uncorrelated with  $\underline{z}$ , with  $\underline{s}$ , and with  $\Delta_{\underline{s}}$ ; in addition,  $\Delta_{\underline{s}}$  is uncorrelated with  $\underline{z}$ . If the second-order moment of  $\Delta_{\underline{z}}$  is upper bounded by  $\epsilon\mathbf{I}_L$ , then the distributionally robust estimator of  $\mathbf{W}$  becomes a kernel ridge regression (i.e., squared- $F$ -norm regularized) method (53). The regularization term becomes  $\text{Tr}[\mathbf{W}\mathbf{F}\mathbf{W}^\top]$ , which is known as the Tikhonov regularizer, if the second-order moment of  $\Delta_{\underline{z}}$  is upper bounded by  $\epsilon\mathbf{F}$  for some  $\mathbf{F} \succeq \mathbf{0}$ .  $\square$

Non-trivial uncertainty sets using the Wasserstein distance or the  $F$ -norm, beyond the diagonal  $\epsilon$ -perturbation (cf. Example 6), for  $\hat{\mathbf{R}}_{\underline{z}}$ ,  $\hat{\mathbf{R}}_{\underline{z}\underline{z}}$ , and  $\hat{\mathbf{R}}_{\underline{s}}$  can be straightforwardly employed and the distributional robustness modeling and analyses remain routine; see Subsection IV-B. Hence, we omit them here.

2) *Multi-Frame Case: Dynamic Channel Evolution:* As in (43), the multi-frame formulation in RKHSs is

$$\min_{\mathbf{W} \in \mathbb{R}^{2M \times L}} \text{Tr} \mathbb{E}_{\underline{\mathbf{x}}, \underline{\mathbf{s}}} [\mathbf{W} \cdot \varphi(\mathbf{x}) - \underline{\mathbf{s}}] [\mathbf{W} \cdot \varphi(\mathbf{x}) - \underline{\mathbf{s}}]^\top + \lambda \cdot \text{Tr}[\mathbf{W} - \mathbf{W}'][\mathbf{W} - \mathbf{W}']^\top, \quad (56)$$

where  $\mathbf{W}'$  denotes the beamformer in the immediately preceding frame and serves as a *prior knowledge* of  $\mathbf{W}$ .

*Claim 3 (Multi-Frame Estimation in RKHS):* The solution of (56) is given by (cf. (48))

$$\begin{aligned} \mathbf{W}_{\text{RKHS-MF}}^* &= [\mathbf{R}_{\underline{z}\underline{s}} + \lambda \mathbf{W}'^\top] [\mathbf{R}_{\underline{z}} + \lambda \mathbf{I}_L]^{-1} \\ &= \left( \frac{1}{L} \underline{\mathbf{S}} \mathbf{K} + \lambda \mathbf{W}'^\top \right) \cdot \left( \frac{1}{L} \mathbf{K}^2 + \lambda \mathbf{I}_L \right)^{-1}, \end{aligned} \quad (57)$$

where  $\lambda \geq 0$  is a tuning parameter to control the similarity between  $\mathbf{W}$  and  $\mathbf{W}'$ ; cf. Claim 1.  $\square$

The remaining distributional robustness modeling and analyses on (56) against the uncertainties in  $\hat{\mathbf{R}}_{\underline{z}}$ ,  $\hat{\mathbf{R}}_{\underline{z}\underline{z}}$ , and  $\hat{\mathbf{R}}_{\underline{s}}$  are technically straightforward; see Subsection IV-C. Therefore, we omit them here.

## B. Neural Networks

With the  $\mathbf{W}$ -parameterization  $\phi_{\mathbf{W}_{[R]}}(\mathbf{x})$  of  $\phi(\mathbf{x})$  in feedforward multi-layer neural networks, i.e., (4), the distributionally robust estimation problem (17) becomes

$$\min_{\mathbf{W}_{[R]}} \max_{\mathbb{P}_{\mathbf{x}, \mathbf{s}} \in \mathcal{U}_{\mathbf{x}, \mathbf{s}}} \text{Tr} \mathbb{E}_{\mathbf{x}, \mathbf{s}} [\phi_{\mathbf{W}_{[R]}}(\mathbf{x}) - \underline{\mathbf{s}}] [\phi_{\mathbf{W}_{[R]}}(\mathbf{x}) - \underline{\mathbf{s}}]^\top, \quad (58)$$

where  $\mathbf{W}_{[R]} := \{\mathbf{W}_1, \mathbf{W}_2, \dots, \mathbf{W}_R\}$  and  $\phi_{\mathbf{W}_{[R]}}(\mathbf{x})$  is defined in (4). Problem (58) is highly nonlinear in both argument  $\mathbf{x}$  and parameter  $\mathbf{W}_{[R]}$ , which is different from the case in reproducing kernel Hilbert spaces where the  $\mathbf{W}_{[R]}$ -linearization features. Hence, problem (58) is too complicated to solve to global optimality. According to [27, Cor. 33], under several technical conditions (plus the boundedness of the feasible region of  $\mathbf{W}_{[R]}$ ), (58) is upper bounded by a spectral-norm-regularized empirical risk minimization problem

$$\begin{aligned} \min_{\mathbf{W}_{[R]}} \frac{1}{L} \sum_{i=1}^L \text{Tr} [\phi_{\mathbf{W}_{[R]}}(\underline{\mathbf{x}}_i) - \underline{\mathbf{s}}_i] [\phi_{\mathbf{W}_{[R]}}(\underline{\mathbf{x}}_i) - \underline{\mathbf{s}}_i]^\top + \\ \lambda' \cdot \sum_{r=1}^R \|\mathbf{W}_r\|_2, \end{aligned} \quad (59)$$

for some regularization coefficient  $\lambda' \geq 0$ , where  $\|\cdot\|_2$  denotes the spectral norm of a matrix (i.e., the induced 2-norm). Eq. (59) rigorously justifies the popular norm regularization method in training neural networks: By reducing the upper bound (59) of (58), the value of (58) can be diminished as well. The regularized ERM problem (59) is reminiscent of the ridge regression and the kernel ridge regression methods in Theorems 2 and 3 for distributional robustness in linear regression and RKHS linear regression, respectively. Supposing that  $\mathbf{W}_{[R]}^*$  is an (approximated, or sub-optimal) solution<sup>5</sup> of (59), then the distributionally robust optimal estimator of the transmitted signal  $\mathbf{s}$  can be obtained as

$$\hat{\mathbf{s}} = \Gamma_M \cdot \phi_{\mathbf{W}_{[R]}^*}(\mathbf{x}).$$

Therefore, in training a neural network for wireless signal estimation, it is recommended to apply the norm regularization methods. Since norms on real spaces are equivalent, (59) can be further upper bounded by

$$\begin{aligned} \min_{\mathbf{W}_{[R]}} \frac{1}{L} \sum_{i=1}^L \text{Tr} [\phi_{\mathbf{W}_{[R]}}(\underline{\mathbf{x}}_i) - \underline{\mathbf{s}}_i] [\phi_{\mathbf{W}_{[R]}}(\underline{\mathbf{x}}_i) - \underline{\mathbf{s}}_i]^\top + \\ \lambda \cdot \sum_{r=1}^R \|\mathbf{W}_r\|, \end{aligned} \quad (60)$$

for any matrix norm  $\|\cdot\|$  and some  $\lambda \geq 0$ ;  $\lambda$  depends on  $\lambda'$  and  $\|\cdot\|$ . As a result, to achieve distributional robustness in training a neural network, any-norm-regularized learning method in (60) can be considered.

<sup>5</sup>Neural networks are hard to be globally optimized.

## VI. EXPERIMENTS

We consider a point-to-point multiple-input-multiple-output (MIMO) wireless communication problem where the transmitter is located at  $[0, 0]$  and the receiver is at  $[500m, 450m]$ . We randomly sample 25 points according to the uniform distribution on the square of  $[0, 500m] \times [0, 500m]$  to denote the scatters' positions; i.e., there exist 25 radio paths. All the source data and codes are available online at GitHub with thorough implementation comments: <https://github.com/Spratm-Asleaf/Beamforming>. In this section, we only present major experimental setups and results; readers can use the shared source codes to explore (or verify) minor ones.

The following eleven methods are implemented in the experiments: 1) **Wiener**: Wiener beamformer (13), upper expression; 2) **Wiener-DL**: Wiener beamformer with diagonal loading (27), upper expression; 3) **Wiener-DR**: Distributionally robust Wiener beamformer (37) and (41); 4) **Wiener-CE**: Channel-estimation-based Wiener beamformer (13), lower expression; 5) **Wiener-CE-DL**: Channel-estimation-based Wiener beamformer with diagonal loading (27), lower expression; 6) **Wiener-CE-DR**: Distributionally robust channel-estimation-based Wiener beamformer (31) and (33); 7) **Capon**: Capon beamformer (28) for  $\epsilon_1 = 0$ ; 8) **Capon-DL**: Capon beamformer with diagonal loading (28); 9) **ZF**: Zero-forcing beamformer where  $\mathbf{W}_{\text{ZF}} := (\hat{\mathbf{H}}^H \hat{\mathbf{H}})^{-1} \hat{\mathbf{H}}^H$  and  $\hat{\mathbf{H}}$  denotes the estimated channel matrix; 10) **Kernel**: Kernel receiver (50) with all  $\epsilon$ 's in (49) equal to zeroes; and 11) **Kernel-DL**: Kernel receiver with diagonal loading (54). Note that the diagonal-loading-based methods are particular cases of distributionally robust beamformers; see, e.g., Examples 1 and 6. The deep-learning-based (DL-based) methods in Subsection V-B are not implemented in this section because they have been deeply studied in our previous publications, e.g., [10], [12]; we only comment on the advantages and disadvantages of DL-based methods compared with the listed eleven methods in Section VII (Conclusions).

When covariance matrix  $\mathbf{P}$  of transmitted signal  $\mathbf{s}$  is unknown for the receiver (e.g., in ISAC systems,  $\mathbf{P}$  needs to vary from one frame to another for sensing),  $\mathbf{P}$  is estimated by the sample covariance matrix  $\hat{\mathbf{P}} = \mathbf{S}\mathbf{S}^H/L$ . The channel matrix  $\mathbf{H}$  is estimated using the minimum mean-squared error method, i.e.,  $\hat{\mathbf{H}} = \mathbf{X}\mathbf{S}^H(\mathbf{S}\mathbf{S}^H)^{-1}$ . Covariance matrix  $\mathbf{R}$  of channel noise  $\mathbf{v}$  is estimated using the least-square method, i.e.,  $\hat{\mathbf{R}} = (\mathbf{X} - \hat{\mathbf{H}}\mathbf{S})(\mathbf{X} - \hat{\mathbf{H}}\mathbf{S})^H/L$ . The matrices  $\hat{\mathbf{P}}$ ,  $\hat{\mathbf{H}}$ , and  $\hat{\mathbf{R}}$  are therefore uncertain compared to their true (but unknown) values  $\mathbf{P}$ ,  $\mathbf{H}$ , and  $\mathbf{R}$ , respectively. The matrices  $\hat{\mathbf{P}}$ ,  $\hat{\mathbf{H}}$ , and  $\hat{\mathbf{R}}$  are used in beamformers such as the channel-estimation-based Wiener beamformer (27), the Capon beamformer, and the zero-forcing beamformer.

The beamformers are determined on the training data set (i.e., pilot data). The performance evaluation method of beamformers is mean-squared estimation error (MSE) on the test data set (i.e., non-pilot communication data); when the transmitted discrete symbols are from constellations, the symbol-error rate (SER) is used. As data-driven machine learning methods, all parameters (e.g., uncertainty quantification coefficients  $\epsilon$ 's) of beamformers can be tuned using the popular

cross-validation (e.g., one-shot cross-validation) method. The parameters can also be empirically tuned to save training times because cross-validation imposes a significant computational burden. This paper mainly uses the empirical tuning method (i.e., trial-and-error) to tune each beamformer to achieve its best average performance. For each test case, the performances are averaged on 200 Monte-Carlo episodes.

**Scenario 1.** We consider the following scenario: the transmitter has four antennas (i.e.,  $M = 4$ ) with unit transmitting power; a communication frame contains 500 non-pilot data (i.e., the size of the testing data set is 500); the channel noises are complex Gaussian. First, we suppose that the transmitting antennas emit continuous-valued complex signals; without loss of generality, Gaussian signals are used in experiments. The performance evaluation measure is therefore the mean-squared error (MSE). The experimental results are shown in Fig. 1.

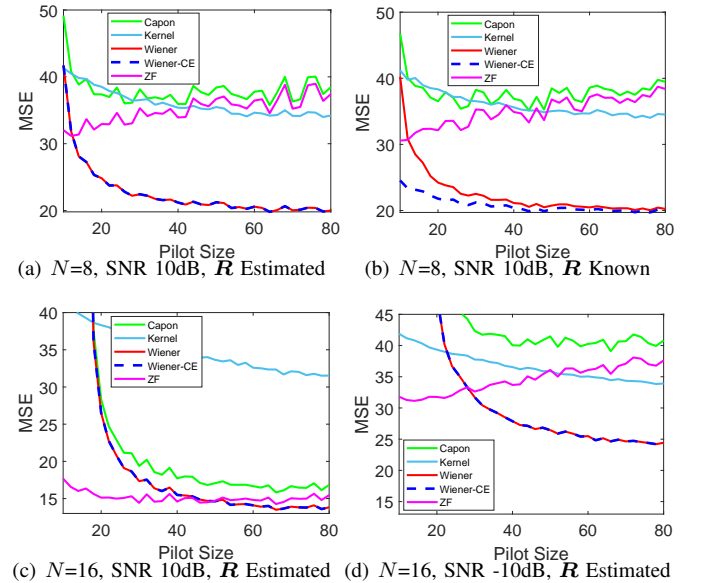


Fig. 1. Testing MSE against training pilot sizes under different numbers of receiving antennas; only non-robust beamformers including non-diagonally-loaded ones are considered. The true value of  $\mathbf{R}$  can be unknown and estimated using pilot data. The signal-to-noise ratio (SNR) is 10dB or  $-10$ dB.

In Fig. 1, for figure clarity, only non-robust beamformers including non-diagonally-loaded ones are considered. From Fig. 1, the following main points can be outlined.

- 1) For a fixed number  $M$  of transmitting antennas, the larger the number  $N$  of receiving antennas, the smaller the MSE; cf. Figs. 1(a) and 1(c). This fact is well-established and is due to the benefit of antenna diversity. In addition, for fixed  $N$  and  $M$ , the higher the SNR, the smaller the MSE; cf. Figs. 1(c) and 1(d); this is also well believed.
- 2) As the pilot size increases, the Wiener beamformer tends to have the best performance because the Wiener beamformer is optimal for the linear Gaussian signal model. When  $\mathbf{R}$  is accurately known, the Wiener-CE beamformer outperforms the general Wiener beamformer (cf. Fig. 1(b)) because the former also exploits the information of the linear signal model in addition to the pilot data, while the latter only utilizes the pilot data. However, when  $\mathbf{R}$  is estimated using the pilot data, the

performances of the general Wiener beamformer and the Wiener-CE beamformer have no significant difference; cf. Figs. 1(a) and 1(c). Therefore, Fig. 1 validates our claim that *channel estimation is not a necessary operation in beamforming and estimation of wireless signals*; recall Subsection III-A3.

- 3) The ZF beamformer tends to be more efficient as  $N$  increases; cf. Figs. 1(a) and 1(c). However, the ZF beamformer becomes less satisfactory when the SNR decreases; cf. Figs. 1(c) and 1(d). The Capon beamformer is also unsatisfactory when  $N$  is small or the SNR is low.
- 4) The kernel beamformer, as a nonlinear method, cannot outperform linear beamformers because, for a linear Gaussian signal model, the optimal beamformer is linear. From the perspective of machine learning, nonlinear methods tend to overfit the limited training samples.

Second, we suppose that the transmitting antennas emit discrete-valued symbols from a constellation that is modulated using quadrature phase-shift keying (QPSK). The performance evaluation measure is therefore the symbol error rate (SER). The experimental results are shown in Fig. 2. We find that all the conclusive main points from Fig. 1 can be obtained from Fig. 2 as well: this validates that *minimizing MSE reduces SER*. In addition, Figs. 2(c) and 2(d) reveal that the Wiener beamformer even slightly works better than the Wiener-CE beamformer when the pilot size is smaller than 15 because the uncertainty in the estimated  $\hat{\mathbf{R}}$ , on the contrary, misleads the latter. Nevertheless, as the pilot size increases, the Wiener-CE beamformer tends to overlap the Wiener beamformer quickly.

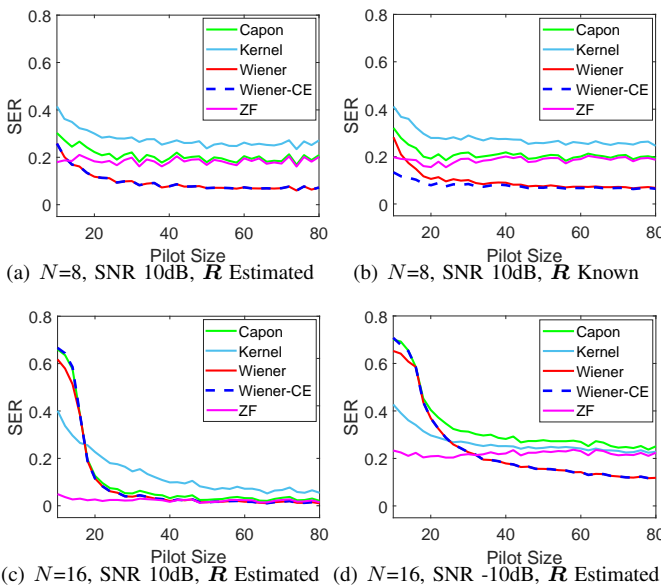


Fig. 2. Testing SER against training pilot sizes under different numbers of receiving antennas; only non-robust beamformers including non-diagonally-loaded ones are considered. The true value of  $\mathbf{R}$  can be unknown and estimated using pilot data. The signal-to-noise ratio (SNR) is 10dB or  $-10$ dB.

**Scenario 2.** Next, we consider another experimental scenario in which impulse channel noises exist. The detailed setups are as follows. The transmitter has four antennas (i.e.,  $M = 4$ ) with unit transmitting power; without loss of

generality, each antenna is assumed to emit continuous-valued complex Gaussian signals. The receiver has eight antennas (i.e.,  $N = 8$ ). The SNR is  $-10$ dB, which is a challenging situation; cf. Figs. 2(c) and 2(d). The channel has impulse noises: i.e., in  $L$  received signals (i.e.,  $[\mathbf{x}_1, \mathbf{x}_2, \dots, \mathbf{x}_L]$ ) that are contaminated by usual complex Gaussian channel noises, 10% of them are also contaminated by uniform noises with the maximum amplitude of 1.5, which is a relatively large value compared to the amplitude of the usual Gaussian channel noises. As in the first scenario, we assume that a communication frame contains 500 non-pilot data. To also disclose the computational times of training beamformers, we employ tables to display the experimental results; see Table I and Appendix H (Table II) of the online supplementary materials.

TABLE I  
RESULTS OF SCENARIO 2 (PILOT SIZE = 20)

Beamformer	MSE	Time	Beamformer	MSE	Time
Wnr	41.42	5.63e-04	Wnr-DL	41.29	2.60e-05
Wnr-DR	38.18	3.51e+00	Wnr-CE	41.42	1.37e-04
Wnr-CE-DL	41.29	4.75e-05	Wnr-CE-DR	41.53	1.33e-04
Capon	86.13	1.15e-04	Capon-DL	85.99	5.23e-05
ZF	75.49	6.89e-05	Kernel	37.20	5.50e-04
Kernel-DL	<b>34.87</b>	1.77e-04			

Wnr: The abbreviation for Wiener.

Time: The training time averaged on 200 Monte-Carlo episodes.

Taking the Wiener beamformer for instance, the averaged MSE for each transmitted symbol is  $41.42/(500 \times 4) = 0.021$ . From Table I, the following main points can be outlined.

- 1) Since the signal model under impulse channel noises is no longer linear Gaussian, the optimal beamformer in the MSE sense must be nonlinear. Therefore, the Kernel and the Kernel-DL methods have the potential to outperform other linear beamformers, i.e., to *suppress outliers*.
- 2) Distributionally robust beamformers (including diagonally loaded ones) can combat the adverse effect introduced by the limited pilot size and several types of uncertainties in the signal model (e.g., outliers). To be specific, for example, all diagonally-loaded beamformers can outperform their original non-diagonally-loaded counterparts; cf. the Wiener and the Wiener-DL methods, the Wiener-CE and the Wiener-CE-DL methods, the Capon and the Capon-DL methods, and the Kernel and the Kernel-DL methods. In addition, the Wiener-DR beamformer (41) using the nontrivial  $F$ -norm uncertainty set can further outperform the Wiener-DL beamformer (27) that simply employs the trivial uncertainty set (26).
- 3) Although the Wiener-DR beamformer has the potential to work better than the Wiener-DL beamformer, it has a significant computational burden, which may not be suitable for timely use in practice especially when the computing resources are limited. Hence, the Wiener-DL beamformer is practically promising (if the pilot size can be improved) because it can provide an excellent balance between the computational burden and the performance.

**Remark on Parameter Tuning.** From experiments on Scenarios 1 and 2, we find that the uncertainty quantification

coefficients  $\epsilon$ 's (e.g., in diagonal loading) can neither be too large nor too small. When  $\epsilon$ 's are too large, the beamformers become overly conservative, while when  $\epsilon$ 's are too small, the beamformers cannot offer sufficient robustness against data scarcity and uncertainties. In both cases of inappropriate  $\epsilon$ 's, the performances of beamformers degrade significantly. Therefore,  $\epsilon$ 's must be carefully tuned in practice, and a rigorous method to tune  $\epsilon$ 's can be the cross-validation method on the training data set (i.e., the pilot data set). If practitioners just pursue satisfaction rather than optimality, the empirical tuning method is recommended to save training time.

## VII. CONCLUSIONS

This paper introduces a unified mathematical framework for beamforming and estimation of wireless signals from the perspective of data-driven machine learning, which reveals that channel estimation is not a necessary operation; the channel-estimation-based beamformers are advantageous only when the pilot size is small and the covariance matrix  $\mathbf{R}$  of the channel noises is (approximately) known. To combat the limited pilot size and several types of uncertainties in the signal model, the distributionally robust (DR) beamforming and estimation framework is then suggested. We prove that the existing diagonal-loading (DL) methods are distributionally robust against the scarcity of pilot data and the uncertainties in the signal model. In addition, we generalize the diagonal-loading methods to achieve better estimation performance (e.g., the DR Wiener beamformer using  $F$ -norm for uncertainty quantification). Experiments suggest that nonlinear beamformers such as the kernel and the kernel-DL methods have the potential when the pilot size is small and/or the signal model is not linear Gaussian. Compared with the kernel and the kernel-DL beamformers, neural-network-based solutions [10], [12] have the stronger expressive capability of nonlinearities, which however are unscalable in the numbers of transmitting and receiving antennas, and significantly more time-consuming in training and more troublesome in tuning hyper-parameters (e.g., the number of layers and the number of neurons in each layer) than the studied eleven beamformers.

## REFERENCES

- [1] T. Lo, H. Leung, and J. Litva, "Nonlinear beamforming," *Electronics Letters*, vol. 4, no. 27, pp. 350–352, 1991.
- [2] S. Yang and L. Hanzo, "Fifty years of MIMO detection: The road to large-scale MIMOS," *IEEE Commun. Surveys Tuts.*, vol. 17, no. 4, pp. 1941–1988, 2015.
- [3] A. M. Elbir, K. V. Mishra, S. A. Vorobyov, and R. W. Heath, "Twenty-five years of advances in beamforming: From convex and nonconvex optimization to learning techniques," *IEEE Signal Processing Mag.*, vol. 40, no. 4, pp. 118–131, 2023.
- [4] S. Chen, S. Tan, L. Xu, and L. Hanzo, "Adaptive minimum error-rate filtering design: A review," *Signal Processing*, vol. 88, no. 7, pp. 1671–1697, 2008.
- [5] S. Chen, A. Wolfgang, C. J. Harris, and L. Hanzo, "Symmetric RBF classifier for nonlinear detection in multiple-antenna-aided systems," *IEEE Trans. Neural Networks*, vol. 19, no. 5, pp. 737–745, 2008.
- [6] A. Navia-Vazquez, M. Martinez-Ramon, L. E. Garcia-Munoz, and C. G. Christodoulou, "Approximate kernel orthogonalization for antenna array processing," *IEEE Trans. Antennas Propagat.*, vol. 58, no. 12, pp. 3942–3950, 2010.
- [7] M. Neinavaie, M. Derakhtian, and S. A. Vorobyov, "Lossless dimension reduction for integer least squares with application to sphere decoding," *IEEE Trans. Signal Processing*, vol. 68, pp. 6547–6561, 2020.
- [8] J. Liao, J. Zhao, F. Gao, and G. Y. Li, "Deep learning aided low complex breadth-first tree search for MIMO detection," *IEEE Trans. Wireless Commun.*, 2023.
- [9] D. A. Awan, R. L. Cavalcante, M. Yukawa, and S. Stanczak, "Robust online multiuser detection: A hybrid model-data driven approach," *IEEE Trans. Signal Processing*, 2023.
- [10] H. Ye, G. Y. Li, and B.-H. Juang, "Power of deep learning for channel estimation and signal detection in OFDM systems," *IEEE Wireless Commun. Lett.*, vol. 7, no. 1, pp. 114–117, 2017.
- [11] H. He, C.-K. Wen, S. Jin, and G. Y. Li, "Model-driven deep learning for MIMO detection," *IEEE Trans. Signal Processing*, vol. 68, pp. 1702–1715, 2020.
- [12] N. Van Huynh and G. Y. Li, "Transfer learning for signal detection in wireless networks," *IEEE Wireless Commun. Lett.*, vol. 11, no. 11, pp. 2325–2329, 2022.
- [13] J. Li, P. Stoica, and Z. Wang, "On robust Capon beamforming and diagonal loading," *IEEE Trans. Signal Processing*, vol. 51, no. 7, pp. 1702–1715, 2003.
- [14] R. G. Lorenz and S. P. Boyd, "Robust minimum variance beamforming," *IEEE Trans. Signal Processing*, vol. 53, no. 5, pp. 1684–1696, 2005.
- [15] X. Zhang, Y. Li, N. Ge, and J. Lu, "Robust minimum variance beamforming under distributional uncertainty," in *2015 IEEE International Conference on Acoustics, Speech and Signal Processing (ICASSP)*. IEEE, 2015, pp. 2514–2518.
- [16] B. Li, Y. Rong, J. Sun, and K. L. Teo, "A distributionally robust minimum variance beamformer design," *IEEE Signal Processing Lett.*, vol. 25, no. 1, pp. 105–109, 2017.
- [17] Y. Huang, W. Yang, and S. A. Vorobyov, "Robust adaptive beamforming maximizing the worst-case SINR over distributional uncertainty sets for random inc matrix and signal steering vector," in *ICASSP 2022-2022 IEEE International Conference on Acoustics, Speech and Signal Processing (ICASSP)*. IEEE, 2022, pp. 4918–4922.
- [18] Y. Huang, H. Fu, S. A. Vorobyov, and Z.-Q. Luo, "Robust adaptive beamforming via worst-case SINR maximization with nonconvex uncertainty sets," *IEEE Trans. Signal Processing*, vol. 71, pp. 218–232, 2023.
- [19] H. Cox, R. Zeskind, and M. Owen, "Robust adaptive beamforming," *IEEE Trans. Acoust., Speech, Signal Processing*, vol. 35, no. 10, pp. 1365–1376, 1987.
- [20] K. Harmanci, J. Tabrikian, and J. L. Krolik, "Relationships between adaptive minimum variance beamforming and optimal source localization," *IEEE Trans. Signal Processing*, vol. 48, no. 1, pp. 1–12, 2000.
- [21] F. Liu, L. Zhou, C. Masouros, A. Li, W. Luo, and A. Petropulu, "Toward dual-functional radar-communication systems: Optimal waveform design," *IEEE Trans. Signal Processing*, vol. 66, no. 16, pp. 4264–4279, 2018.
- [22] J. A. Zhang, F. Liu, C. Masouros, R. W. Heath, Z. Feng, L. Zheng, and A. Petropulu, "An overview of signal processing techniques for joint communication and radar sensing," *IEEE J. Select. Topics Signal Processing*, vol. 15, no. 6, pp. 1295–1315, 2021.
- [23] Y. Xiong, F. Liu, Y. Cui, W. Yuan, T. X. Han, and G. Caire, "On the fundamental tradeoff of integrated sensing and communications under Gaussian channels," *IEEE Trans. Inform. Theory*, 2023.
- [24] K. P. Murphy, *Machine Learning: A Probabilistic Perspective*. MIT Press, 2012.
- [25] C. M. Bishop and N. M. Nasrabadi, *Pattern Recognition and Machine Learning*. Springer, 2006, vol. 4, no. 4.
- [26] G. Li and J. Ding, "Towards understanding variation-constrained deep neural networks," *IEEE Trans. Signal Processing*, vol. 71, pp. 631–640, 2023.
- [27] S. Shafeezadeh-Abadeh, D. Kuhn, and P. M. Esfahani, "Regularization via mass transportation," *Journal of Machine Learning Research*, vol. 20, no. 103, pp. 1–68, 2019.
- [28] M. Staib and S. Jegelka, "Distributionally robust optimization and generalization in kernel methods," *Advances in Neural Information Processing Systems*, vol. 32, 2019.
- [29] S. Wang, "Distributionally robust state estimation for jump linear systems," *IEEE Trans. Signal Processing*, 2023.
- [30] D. Kuhn, P. M. Esfahani, V. A. Nguyen, and S. Shafeezadeh-Abadeh, "Wasserstein distributionally robust optimization: Theory and applications in machine learning," in *Operations Research & Management Science in the Age of Analytics*. Informs, 2019, pp. 130–166.
- [31] K. Vu, J. C. Snyder, L. Li, M. Rupp, B. F. Chen, T. Khelif, K.-R. Müller, and K. Burke, "Understanding kernel ridge regression: Common behaviors from simple functions to density functionals," *International Journal of Quantum Chemistry*, vol. 115, no. 16, pp. 1115–1128, 2015.

## Supplementary Materials

### APPENDIX A STRUCTURED REPRESENTATION OF NONLINEAR FUNCTIONS

In Section II, we have reviewed two popular frameworks for representing (nonlinear) functions: reproducing kernel Hilbert spaces (RKHS) and neural network function spaces (NNFS). Typical kernel functions  $\ker(\cdot, \cdot)$  to define RKHSs include

- 1) Gaussian kernel,
- 2) Matern kernel,
- 3) Linear kernel,
- 4) Laplacian kernel,
- 5) Polynomial kernel.

Mathematical details of these kernel functions can be found in [24, Subsec. 14.2], [27, Ex. 1]. Typical activation functions  $\sigma(\cdot)$  to define NNFSs include

- 1) Hyperbolic tangent (i.e.,  $\tanh$ ) function,
- 2) Softmax function,
- 3) Sigmoid function,
- 4) Rectified linear unit (ReLU) function,
- 5) Exponential linear unit (ELU) function,
- 6) Linear function.

Mathematical details of these activation functions can be found in [27, Ex. 2].

### APPENDIX B DETAILS ON REAL-SPACE SIGNAL REPRESENTATION

We have

$$\begin{aligned} \mathbf{R}_{\underline{x}} &:= \mathbb{E}_{\underline{x}\underline{x}^T} = \frac{1}{2} \begin{bmatrix} \text{Re}(\mathbf{R}_x + \mathbf{C}_x) & \text{Im}(-\mathbf{R}_x + \mathbf{C}_x) \\ \text{Im}(\mathbf{R}_x + \mathbf{C}_x) & \text{Re}(\mathbf{R}_x - \mathbf{C}_x) \end{bmatrix}. \\ \mathbf{R}_{\underline{s}} &:= \mathbb{E}_{\underline{s}\underline{s}^T} = \frac{1}{2} \begin{bmatrix} \text{Re}(\mathbf{P} + \mathbf{C}) & \text{Im}(-\mathbf{P} + \mathbf{C}) \\ \text{Im}(\mathbf{P} + \mathbf{C}) & \text{Re}(\mathbf{P} - \mathbf{C}) \end{bmatrix}, \end{aligned}$$

and

$$\mathbf{R}_{\underline{v}} := \mathbb{E}_{\underline{v}\underline{v}^T} = \frac{1}{2} \begin{bmatrix} \text{Re } \mathbf{R} & \text{Im } -\mathbf{R} \\ \text{Im } \mathbf{R} & \text{Re } \mathbf{R} \end{bmatrix}.$$

Note that notationally  $\mathbf{P} := \mathbf{R}_s$ ,  $\mathbf{C} := \mathbf{C}_s$ , and  $\mathbf{R} := \mathbf{R}_v$ . Note also that the following identities hold:  $\mathbf{R}_x = \mathbf{H}\mathbf{R}_s\mathbf{H}^H + \mathbf{R}_v$ ,  $\mathbf{C}_x = \mathbf{H}\mathbf{C}_s\mathbf{H}^T$ ,  $\mathbf{R}_{\underline{x}} = \underline{\mathbf{H}} \cdot \mathbf{R}_{\underline{s}} \cdot \underline{\mathbf{H}}^T + \mathbf{R}_{\underline{v}}$ , and  $\mathbf{R}_{\underline{x}\underline{s}} = \underline{\mathbf{H}} \cdot \mathbf{R}_{\underline{s}}$ .

### APPENDIX C

#### EXTENSIVE READING ON DISTRIBUTIONAL UNCERTAINTY

We use (7) and (15) as examples to illustrate the concepts. Supposing that  $\phi^*$  solves the true problem (7) and  $\phi_{\text{ERM}}^*$  solves the surrogate problem (15), we have

$$\begin{aligned} \min_{\phi} \text{Tr} \mathbb{E}_{(\mathbf{x}, \mathbf{s}) \sim \mathbb{P}_{\mathbf{x}, \mathbf{s}}} [\phi(\mathbf{x}) - \mathbf{s}] [\phi(\mathbf{x}) - \mathbf{s}]^H \\ = \text{Tr} \mathbb{E}_{(\mathbf{x}, \mathbf{s}) \sim \mathbb{P}_{\mathbf{x}, \mathbf{s}}} [\phi^*(\mathbf{x}) - \mathbf{s}] [\phi^*(\mathbf{x}) - \mathbf{s}]^H \\ \leq \text{Tr} \mathbb{E}_{(\mathbf{x}, \mathbf{s}) \sim \mathbb{P}_{\mathbf{x}, \mathbf{s}}} [\phi_{\text{ERM}}^*(\mathbf{x}) - \mathbf{s}] [\phi_{\text{ERM}}^*(\mathbf{x}) - \mathbf{s}]^H. \end{aligned} \quad (61)$$

To clarify further, the testing error in the last line (evaluated at the true distribution  $\mathbb{P}_{\mathbf{x}, \mathbf{s}}$ ) of the learned estimator  $\phi_{\text{ERM}}^*$  may be (much) larger than the optimal error in the first two lines,

although  $\phi_{\text{ERM}}^*$  has the smallest training error (evaluated at the nominal distribution  $\hat{\mathbb{P}}_{\mathbf{x}, \mathbf{s}}$ ), i.e.,

$$\begin{aligned} \min_{\phi} \text{Tr} \mathbb{E}_{(\mathbf{x}, \mathbf{s}) \sim \hat{\mathbb{P}}_{\mathbf{x}, \mathbf{s}}} [\phi(\mathbf{x}) - \mathbf{s}] [\phi(\mathbf{x}) - \mathbf{s}]^H \\ = \min_{\phi} \text{Tr} \frac{1}{L} \sum_{i=1}^L [\phi(\mathbf{x}_i) - \mathbf{s}_i] [\phi(\mathbf{x}_i) - \mathbf{s}_i]^H \\ = \text{Tr} \frac{1}{L} \sum_{i=1}^L [\phi_{\text{ERM}}^*(\mathbf{x}_i) - \mathbf{s}_i] [\phi_{\text{ERM}}^*(\mathbf{x}_i) - \mathbf{s}_i]^H \\ \leq \text{Tr} \frac{1}{L} \sum_{i=1}^L [\phi^*(\mathbf{x}_i) - \mathbf{s}_i] [\phi^*(\mathbf{x}_i) - \mathbf{s}_i]^H. \end{aligned} \quad (62)$$

In the terminologies of machine learning, the difference between the testing error and the training error, i.e.,

$$\begin{aligned} \text{Tr} \mathbb{E}_{(\mathbf{x}, \mathbf{s}) \sim \mathbb{P}_{\mathbf{x}, \mathbf{s}}} [\phi_{\text{ERM}}^*(\mathbf{x}) - \mathbf{s}] [\phi_{\text{ERM}}^*(\mathbf{x}) - \mathbf{s}]^H - \\ \text{Tr} \mathbb{E}_{(\mathbf{x}, \mathbf{s}) \sim \hat{\mathbb{P}}_{\mathbf{x}, \mathbf{s}}} [\phi_{\text{ERM}}^*(\mathbf{x}) - \mathbf{s}] [\phi_{\text{ERM}}^*(\mathbf{x}) - \mathbf{s}]^H \\ = \text{Tr} \mathbb{E}_{\mathbf{x}, \mathbf{s}} [\phi_{\text{ERM}}^*(\mathbf{x}) - \mathbf{s}] [\phi_{\text{ERM}}^*(\mathbf{x}) - \mathbf{s}]^H - \\ \text{Tr} \frac{1}{L} \sum_{i=1}^L [\phi_{\text{ERM}}^*(\mathbf{x}_i) - \mathbf{s}_i] [\phi_{\text{ERM}}^*(\mathbf{x}_i) - \mathbf{s}_i]^H \end{aligned}$$

is called the *generalization error* of  $\phi_{\text{ERM}}^*$ ; the difference between the testing error and the optimal error, i.e.,

$$\begin{aligned} \text{Tr} \mathbb{E}_{\mathbf{x}, \mathbf{s}} [\phi_{\text{ERM}}^*(\mathbf{x}) - \mathbf{s}] [\phi_{\text{ERM}}^*(\mathbf{x}) - \mathbf{s}]^H - \\ \text{Tr} \mathbb{E}_{\mathbf{x}, \mathbf{s}} [\phi^*(\mathbf{x}) - \mathbf{s}] [\phi^*(\mathbf{x}) - \mathbf{s}]^H \end{aligned}$$

is called the *excess risk* of  $\phi_{\text{ERM}}^*$ .

In the practice of machine learning, we want to reduce both the generalization error and the excess risk. Most attention in the literature has been particularly paid to controlling generalization errors. To be specific, an upper bound of the true cost  $\text{Tr} \mathbb{E}_{(\mathbf{x}, \mathbf{s}) \sim \mathbb{P}_{\mathbf{x}, \mathbf{s}}} [\phi(\mathbf{x}) - \mathbf{s}] [\phi(\mathbf{x}) - \mathbf{s}]^H$  is first found and then minimize the upper bound: by minimizing the upper bound, the true cost can also be reduced. For technical details, see Fact 1.

### APPENDIX D WASSERSTEIN DISTANCE AND MAXIMUM MEAN DISCREPANCY DISTANCE

Consider two distributions (probability measures)  $\mathbb{P}_{\mathbf{x}}$  and  $\mathbb{P}_{\mathbf{y}}$  on the same measurable space  $(\Xi, \mathcal{B}_{\Xi})$  where  $\mathcal{B}_{\Xi}$  is the Borel  $\sigma$ -algebra on the set  $\Xi$ . The Wasserstein distance  $d_{\text{W}}$  between  $\mathbb{P}_{\mathbf{x}}$  and  $\mathbb{P}_{\mathbf{y}}$  is defined as [27, Def. 2]

$$d_{\text{W}}(\mathbb{P}_{\mathbf{x}}, \mathbb{P}_{\mathbf{y}}) := \inf_{\Pi} \int_{\Xi \times \Xi} d(\mathbf{x}, \mathbf{y}) \Pi(d\mathbf{x}, d\mathbf{y}),$$

where  $d$  is a metric on  $\Xi$  and  $\Pi$  is a joint distribution of  $\mathbf{x}$  and  $\mathbf{y}$ ;  $\Xi$  is a coupling of  $\mathbb{P}_{\mathbf{x}}$  and  $\mathbb{P}_{\mathbf{y}}$ : i.e., the marginal distributions induced by  $\Pi$  is  $\mathbb{P}_{\mathbf{x}}$  and  $\mathbb{P}_{\mathbf{y}}$ .

The maximum mean discrepancy (MMD) distance  $d_{\text{MMD}}$  between  $\mathbb{P}_{\mathbf{x}}$  and  $\mathbb{P}_{\mathbf{y}}$  in the reproducing kernel Hilbert space (RKHS)  $\mathcal{H}$  is defined as [28, Def. 2.1]

$$d_{\text{MMD}}(\mathbb{P}_{\mathbf{x}}, \mathbb{P}_{\mathbf{y}}) := \sup_{f \in \mathcal{H}: \|f\|_{\mathcal{H}} \leq 1} [\mathbb{E}_{\mathbf{x}} f(\mathbf{x}) - \mathbb{E}_{\mathbf{y}} f(\mathbf{y})],$$

where  $\|\cdot\|_{\mathcal{H}}$  is a norm on  $\mathcal{H}$  [24, p. 539].

APPENDIX E  
PROOF OF THEOREM 1

*Proof:* Since  $\mathbf{R}_{x,1} \succeq \mathbf{R}_{x,2}$ , we have

$$\begin{bmatrix} \mathbf{R}_s & \mathbf{R}_{xs}^H \\ \mathbf{R}_{xs} & \mathbf{R}_{x,1} \end{bmatrix} - \begin{bmatrix} \mathbf{R}_s & \mathbf{R}_{xs}^H \\ \mathbf{R}_{xs} & \mathbf{R}_{x,2} \end{bmatrix} = \begin{bmatrix} \mathbf{0} & \mathbf{0} \\ \mathbf{0} & \mathbf{R}_{x,1} - \mathbf{R}_{x,2} \end{bmatrix} \succeq \mathbf{0}.$$

According to the properties of the Schur complement, we have  $f(\mathbf{R}_{x,1}) \geq f(\mathbf{R}_{x,2})$ .  $\square$

APPENDIX F  
PROOF OF PROPOSITION 1

*Proof:* Problem (35) is equivalent to

$$\begin{aligned} & \max_{t, \mathbf{R}_x, \mathbf{V}, \mathbf{U}} \quad t \\ \text{s.t.} \quad & \text{Tr}[-\mathbf{V} + \mathbf{R}_s] \geq t \\ & \mathbf{V} \succeq \mathbf{R}_{xs}^H \mathbf{R}_x^{-1} \mathbf{R}_{xs} \\ & \text{Tr}[\mathbf{R}_x + \hat{\mathbf{R}}_x - 2\mathbf{U}] \leq \epsilon_1^2 \\ & \hat{\mathbf{R}}_x^{1/2} \mathbf{R}_x \hat{\mathbf{R}}_x^{1/2} \succeq \mathbf{U}^2 \\ & t \geq 0 \\ & \mathbf{R}_x \succeq 0, \quad \mathbf{R}_x = \mathbf{R}_x^H \\ & \mathbf{V} \succeq 0, \quad \mathbf{V} = \mathbf{V}^H \\ & \mathbf{U} \succeq 0, \quad \mathbf{U} = \mathbf{U}^H. \end{aligned}$$

Then, by applying the Schur complement, we have (36), which completes the proof.  $\square$

APPENDIX G  
PROOF OF PROPOSITION 3

*Proof:* Letting  $\underline{\mathbf{z}} := \varphi(\underline{\mathbf{x}})$ , (46) can be rewritten as

$$\min_{\mathbf{W} \in \mathbb{R}^{2M \times 2N}} \max_{\mathbb{P}_{\underline{\mathbf{z}}, \underline{\mathbf{s}}} \in \mathcal{U}_{\underline{\mathbf{z}}, \underline{\mathbf{s}}}} \text{Tr} \mathbb{E}_{\underline{\mathbf{z}}, \underline{\mathbf{s}}} [\mathbf{W} \underline{\mathbf{z}} - \underline{\mathbf{s}}][\mathbf{W} \underline{\mathbf{z}} - \underline{\mathbf{s}}]^T. \quad (63)$$

Tantamount to the distributionally robust beamforming problem (19), problem (63) reduces to (47) where

$$\hat{\mathbf{R}}_{\underline{\mathbf{z}}} := \frac{1}{L} \sum_{i=1}^L \underline{\mathbf{z}}_i \underline{\mathbf{z}}_i^T = \frac{1}{L} \sum_{i=1}^L \varphi(\underline{\mathbf{x}}_i) \varphi^T(\underline{\mathbf{x}}_i) = \frac{1}{L} \mathbf{K}^2,$$

$$\hat{\mathbf{R}}_{\underline{\mathbf{z}}\underline{\mathbf{s}}} := \frac{1}{L} \sum_{i=1}^L \underline{\mathbf{z}}_i \underline{\mathbf{s}}_i^T = \frac{1}{L} \sum_{i=1}^L \varphi(\underline{\mathbf{x}}_i) \cdot \underline{\mathbf{s}}_i^T = \frac{1}{L} \mathbf{K} \underline{\mathbf{S}}^T,$$

$$\hat{\mathbf{R}}_{\underline{\mathbf{s}}} := \frac{1}{L} \sum_{i=1}^L \underline{\mathbf{s}}_i \underline{\mathbf{s}}_i^T = \frac{1}{L} \sum_{i=1}^L \underline{\mathbf{s}}_i \cdot \underline{\mathbf{s}}_i^T = \frac{1}{L} \underline{\mathbf{S}} \underline{\mathbf{S}}^T,$$

and

$$\mathbf{K} := [\varphi(\underline{\mathbf{x}}_1), \varphi(\underline{\mathbf{x}}_2), \dots, \varphi(\underline{\mathbf{x}}_L)] \in \mathbb{R}^{L \times L}.$$

Note that  $\mathbf{K}$  is invertible. The rest statements are due to Lemma 1.  $\square$

TABLE II  
RESULTS OF SCENARIO 2 (PILOT SIZE = 10)

Beamformer	MSE	Time	Beamformer	MSE	Time
Wnr	80.59	6.96e-04	Wnr-DL	77.16	3.31e-05
Wnr-DR	51.35	3.67e+00	Wnr-CE	80.59	4.40e-04
Wnr-CE-DL	77.16	6.37e-05	Wnr-CE-DR	80.72	4.84e-04
Capon	98.31	4.05e-04	Capon-DL	95.56	6.91e-05
ZF	59.11	3.41e-04	Kernel	42.42	8.41e-04
Kernel-DL	<b>40.85</b>	9.20e-05			

APPENDIX H  
ADDITIONAL EXPERIMENTAL RESULTS ON SCENARIO 2

In Section VI (in particular, Table I of Experiments) of the main body of the paper, we present the experimental results under the pilot data size of 20. In this appendix, we display the results under the pilot data size of 10.

As we can see from Table I and Table II, a larger number of pilot data benefits the estimation performances of wireless signals. In addition, the diagonal loading operation can significantly improve the estimation performances especially when the pilot data size is relatively small. Moreover, nonlinear beamformers are preferable over linear ones when impulse channel noises exist.